AD NUMBER

AD844307

NEW LIMITATION CHANGE

TO

Approved for public release, distribution unlimited

FROM

Distribution authorized to U.S. Gov't. agencies and their contractors; Critical Technology; OCT 1968. Other requests shall be referred to Air Force Rome Air Development Center, Griffiss AFB, NY.

AUTHORITY

radc, usaf, ltr, 17 sep 1971

DISCLAIMER NOTICE

THIS DOCUMENT IS BEST QUALITY PRACTICABLE. THE COPY FURNISHED TO DTIC CONTAINED A SIGNIFICANT NUMBER OF PAGES WHICH DO NOT REPRODUCE LEGIBLY.

RADC-TR- 68-243
Final Report

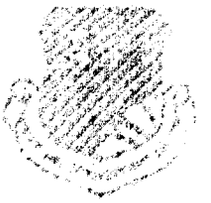

METALLIZATION FAILURES IN INTEGRATED CIRCUITS

James Block
Motorola, Incorporated

TECHNICAL REPORT NO. RADC-TR- 68-243
October 1968

Rome Air Development Center
Air Force Systems Command
Griffiss Air Force Base, New York

[illegible] drawings, specifications, or other data are used for any purpose other [illegible] related government procurement operation, the government thereby incurs [illegible] liability nor any obligation whatsoever; and the fact that the government may have [illegible], furnished, or in any way supplied the said drawings, specifications, or other [illegible] is not to be regarded, by implication or otherwise, as in any manner licensing the [illegible] or any other person or corporation, or conveying any rights or permission to manu[illegible], use, or sell any patented invention that may in any way be related thereto.

METALLIZATION FAILURES IN INTEGRATED CIRCUITS

James Black

Motorola, Incorporated

AFLC, GAFB, N.Y., 13 Nov 68-164

FOREWORD

This report was prepared by the Semiconductor Products Division of Motorola, Inc., Phoenix, Arizona, on Air Force Contract F30602-67-C-0166, Project 5519, Task 551906. The work was administered by Rome Air Development Center, Griffiss Air Force Base, New York, under Project Engineer, Mr. John Bart, EMERP.

The studies presented cover the period from 28 December 1966 to 27 April 1968. The work was performed by the Applied Science Department under the direction of Dr. I.A. Lesk with Mr. Jim Black as Project Leader.

Information in this report is embargoed under the provisions of the U.S. Mutual Security Acts of 1949.

This Technical Report has been reviewed and is approved.

John J. Bart

Approved: JOHN J. BART
Reliability Physics Section
Reliability Branch

William P. Bartke

Approved: WILLIAM P. ESTKE
Chief, Engineering Division

FOR THE COMMANDER: Irving J. Gabelman
IRVING J. GABELMAN
Chief, Advanced Studies Group

ABSTRACT

The activation energy for the mass transport of aluminum by momentum exchange with conducting electrons has been obtained and equations relating temperature, current density, film structure and film geometry to conductor life are presented. The conductor lifetime is shortened if thermal gradients, current density gradients or compositional gradients exist. Void formation at a compositional gradient where electrons leave silicon and enter aluminum has been qualitatively studied. Also, it is shown that hillocks and whiskers of aluminum form at aluminum-silicon interfaces when electrons leave aluminum and enter silicon. Etch pit growth into silicon at silicon-aluminum contacts carrying high current densities where electrons leave the silicon and enter aluminum have been qualitatively studied. Two concurrent mechanisms leading to the formation of these etch pits are: (1) the dissolution of silicon into aluminum to reach near saturation, and (2) the transport of the dissolved silicon ions down the aluminum and away from the interface by momentum exchange with conducting electrons. A microscopic study of aluminum wires containing 1-percent silicon is presented showing gross structural changes when stressed at elevated current densities. Silicon is also shown to be transported down the wires in the direction of electron flow. Equations relating the rate of penetration of aluminum into silicon dioxide to temperature are presented. This reaction is shown to be unimportant as a failure mode at normal device operating temperatures of 200°C and below.

TABLE OF CONTENTS

TABLE OF CONTENTS (Cont'd.)

LIST OF ILLUSTRATIONS

LIST OF ILLUSTRATIONS (Cont'd.)

LIST OF ILLUSTRATIONS (Cont'd.)

LIST OF ILLUSTRATIONS (Cont'd.)

LIST OF TABLES

EXPLANATION

The purpose of this work was the study of several mechanisms of failures associated with the aluminum metallization system. In an attempt to isolate some of these particular physical reactions, special test structures were used to study the properties of the aluminum film itself, the aluminum-silicon contact area and the aluminum-silicon dioxide interface.

Significant quantitative results were obtained in two major areas of this program:

a. Kinetic relationships were developed describing the time to failure of aluminum films as a result of mass transport of aluminum by momentum exchange with conduction electrons.

b. A rate equation for the penetration of aluminum into thermally grown silicon dioxide was also determined.

Experimental difficulties were encountered in obtaining kinetic information concerning the interaction of silicon and aluminum. This problem was qualitatively studied using secondary electron scanning microscopy. This technique was also successfully used to elucidate the cause of aluminum wire failures when passing high current density at elevated temperatures.

This first attempt at studying electromigration in aluminum did not include the effects of material, temperature or current density gradients which shorten conductor lifetime. Therefore, the lifetimes which can be predicted from the equations in Section 2.1 of this report are optimistic.

It is recommended that a quantitative investigation of the effects of these gradients be considered. This would yield more meaningful information to the designer of integrated circuits where all factors are present.

John J. Hart
JOHN J. HART
Reliability Physics Section
Reliability Branch

SECTION I

1.0 INTRODUCTION

Six potential failure modes involving aluminum as the metallization material for semiconductor devices have been investigated in an attempt to obtain a better understanding of the processes involved and to obtain equations which relate device failure to known physical parameters. This information should enable the construction of reliable devices with predictable lifetimes. The processes which have been investigated are:

(1) The Mass Transport of Aluminum by Momentum Exchange with Conducting Electrons.
(2) The Mass Transport of Aluminum at Aluminum-Silicon Contacts.
(3) Etch Pit Growth in Silicon due to the Mass Transport of Silicon through Aluminum by Momentum Exchange with Conducting Electrons.
(4) A Microscopic Study of Aluminum-1-percent Silicon Wire Failure.
(5) The Reaction Between Aluminum and Silicon Dioxide.
(6) The Dissolution of Silicon into Aluminum.

The first of these becomes an important failure mode commonly found in high power devices and integrated circuits where aluminum conductors carry current densities in excess of 10^5 amperes per square centimeter at temperatures above 100°C. The mode of failure is an open circuit caused by the movement of aluminum ions in the direction of electron flow. This failure mode is enhanced when a thermal gradient, a current gradient or a compositional gradient exists in the conductor. The effect of a compositional gradient when electrons flow from silicon into aluminum or from aluminum into silicon is the subject of the second study.

The third subject deals with the growth of etch pits into silicon at high current density silicon-aluminum contacts where electrons leave the silicon and enter, the aluminum conductor. The etch pits form by the dissolution of silicon into aluminum and the transport of silicon away from the interface by momentum exchange between conducting electrons and the dissolved silicon. The failure mode is the growth of an etch pit through a shallow junction resulting in a shorted junction.

Photomicrographs of aluminum-1-percent silicon wires which have been stressed at elevated temperature, and current densities are presented. The dissolved silicon is seen to be transported through the aluminum in the direction of electron flow.

Aluminum reacts with silicon dioxide to reduce it to silicon at elevated temperatures. Aluminum can penetrate through thin films of SiO_2 by means of this reaction and could result in device failure by an electrical short. This reaction was the subject of the fifth study.

The last subject presented was an attempt to determine the solid-solubility curve for the dissolution of pure silicon into pure aluminum. Etch pits can form by this process in silicon at silicon aluminum interfaces when the couple is heated. The best data available was obtained with impure materials in 1928 and should be updated.

Most of the effort of this 15-month program was devoted to subjects (1) and (5) which resulted in the generation of equations which enable the prediction of failure by these processes. The other subjects studied resulted in a qualitative understanding of the processes involved. No results were obtained in the last subject studied due to experimental difficulties.

SECTION II

2.0 ANALYSIS OF WORK

2.1 MASS TRANSPORT OF ALUMINUM BY MOMENTUM EXCHANGE WITH CONDUCTING ELECTRONS

A failure mode commonly found in high power devices and integrated circuits appears when aluminum conductors carry current densities in excess of 10^5 amperes per square centimeter at temperatures above 100°C. The mode of failure is an open circuit caused by the movement of aluminum ions in the direction of electron flow. Voids in the metal, resulting from this process, tend to grow in a direction normal to the current flow. The effect is an accumulative one increasing the local current density in the region of the void, thus accelerating the process. The end result is a void extending entirely across the film, interrupting the current flow. This frequently occurs in emitter stripes where the stripe thickness is reduced as it extends over a step in the glass surface. Under the step at this point there generally exists a junction in the silicon which dissipates power, thus aggravating the situation by increasing the local temperature.

Figure 1(a) shows a photomicrograph of a 1/2-mil-wide aluminum stripe after it had been stressed at a current density of 1.5×10^6 A/cm^2 at 190°C. Voids are shown growing at the edges and in the center of the film. Also nodules and crystallites of aluminum grow (out of focus) from the film appearing as dark areas. One void has extended nearly half way across the conducting stripe. Aluminum ions are transported away from certain crystallites and cluster at other sites growing well defined crystals or nondescript nodules. Nodule or crystal growth appears downstream in terms of

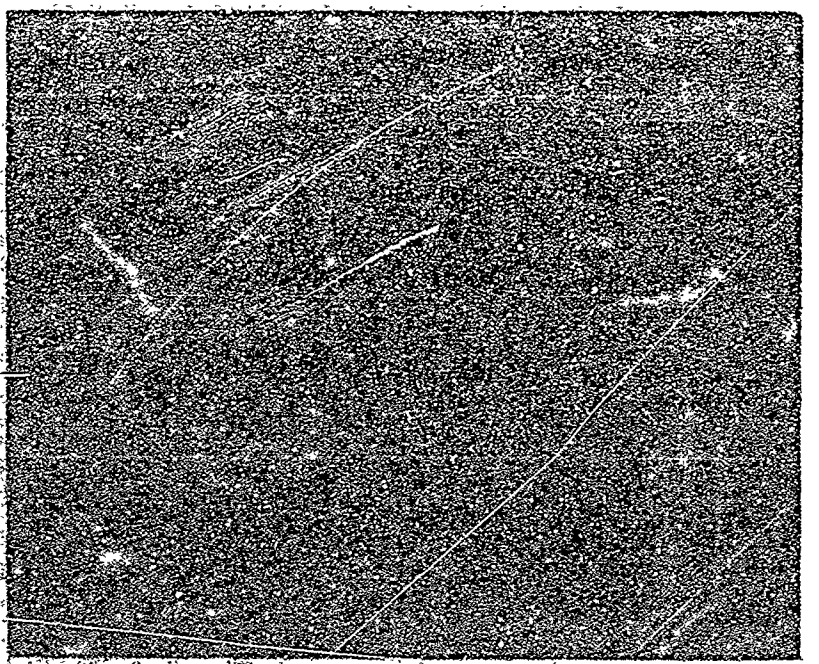

(1400X)

(a)

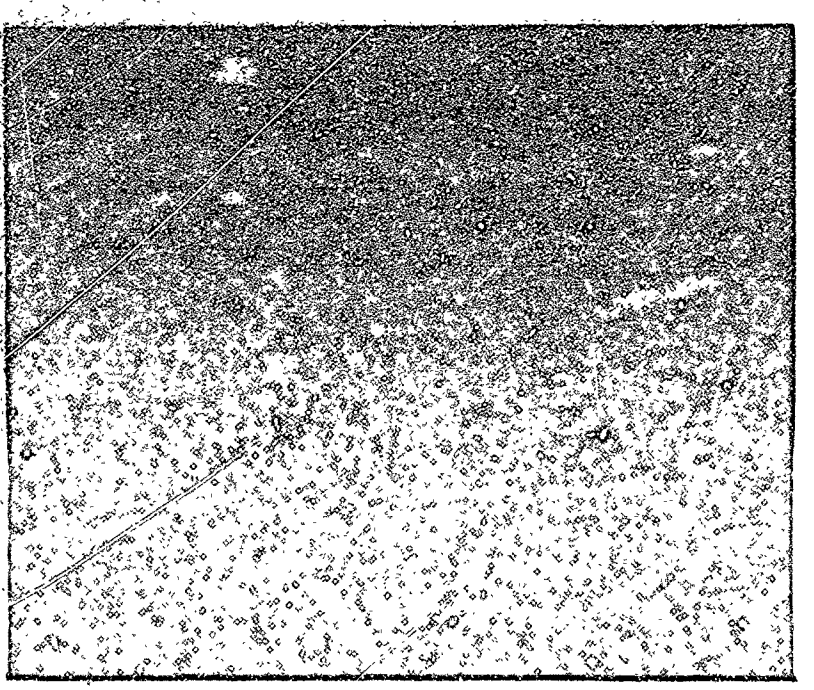

(1400X)

(b)

Figure 1. Stressed Aluminum Films Showing Voids and Crystal Growth

electron flow from voids. The voids and growth regions are rather uniformly distributed over the length of the conductor stripe when the entire stripe is at an elevated temperature and when there are no gradients in current density or film composition.

Figure 1(b) shows extensive surface reordering and a large crystalline whisker of aluminum extends roughly in the plane of the film. A large void also appears along one edge of the film near the center of the picture.

Figure 2(a) is a photomicrograph of a current stressed large grained aluminum film showing the characteristic angular void formation as well as a large whisker growing slightly out of the plane of focus of the picture. The heavy dark spots are also hillocks out of focus. This film was stressed at a current density of 1.2×10^6 A/cm^2 at a film temperature of 186°C for 47 hours.

A view of a similarly stressed film at lower magnification is shown in Figure 2(b) where several whiskers appear. One of these has twinned and then retwinned to grow again in its original direction.

Professor Huntington and co-workers at the Rensselaer Polytechnic Institute have studied the current induced motion of surface scratches on bulk metals. [1,2,3] They have generally

---

(1) R. V. Penney, "Current-Induced Mass Transport in Aluminum," J. Phys. Chem. Solids, 1964, Vol. 25, pp. 334-335.

(2) H. B. Huntington and A. R. Grone, "Current-Induced Marker Motion in Gold Wires," J. Phys. Chem. Solids, 1961, Vol. 20, Nos. 1/2, pp. 76-87.

(3) A. R. Grone, "Current-Induced Marker Motion in Copper, "J. Phys. Chem. Solids, 1961, Nos. 1/2, pp. 88-93.

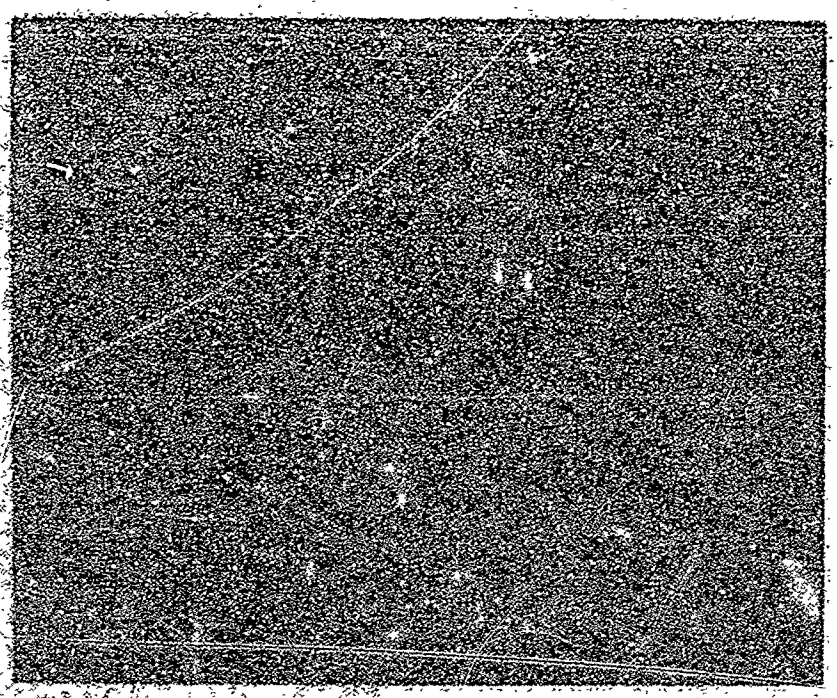

(a)

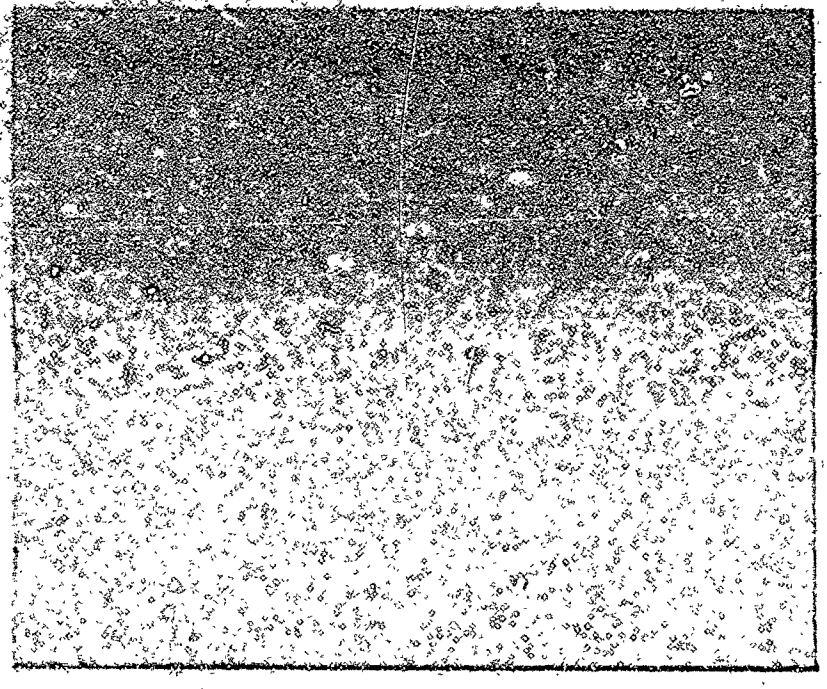

(b)

Figure 2. Stressed Aluminum Films Showing Voids and Crystal Growth

concluded that metal ions which are thermally "activated" (lifted out of the potential well associated with the metal crystal lattic and free to move back into their original potential well or into other potential wells associated with the crystal or neighboring crystals) are acted on by two opposing forces in an electrically conducting metal:

(a) The electric field applied to the conductor will exert a force on the activated ion in the direction opposite to electron flow.

(b) The rate of momentum exchange between the conducting electrons colliding with the activated metal ions will exert a force on the metal ion in the direction of electron flow.

The ion drifts, then, in the direction of the predominating force which at moderate temperatures for the metals investigated is in the direction of electron flow. Metal ions are observed to travel toward the positive end of the conductor while vacancies move toward the negative end. Scratch marks on bulk metal behave as vacancies and are, therefore, observed to move along the surface of the conductor in the direction of the negative terminal.

The activation energy for the velocity of scratch motion in the bulk materials observed by the Rensselaer Polytechnic Institute Group was the same as the activation energy for the lattice self-diffusion of the metals. The velocity of scratch motion was also concluded to be a direct function of current density; however only a small variation in current density was reported in their experiments.

Based upon the above work, an experiment was designed to study the failure rate of long thin aluminum film conductor stripes operated at various current densities and temperatures. Since the aluminum films were formed by the condensation of the vapor in a vacuum ambient, it was anticipated that the activation energy for the failure mode would be less than that of bulk aluminum and highly dependent upon the degree of crystalline order of the film.

Highly polycrystalline films formed by vacuum deposition from tungsten filaments onto cold substrates were suspected of exhibiting very low activation energies due to grain-boundary diffusion and surface diffusion. Well ordered films deposited on heated substrates and possessing large area crystallites should exhibit a substantial activation energy for the failure mode, being depressed from the activation energy due to lattic diffusion mainly by surface diffusion which, for thin films, is important because of their large surface-to-volume ratio. Films deposited with high crystalline order and coated with a glass film in an attempt to reduce the surface diffusion were expected to possess an activation energy for this failure mode approaching that for the lattice self-diffusion of aluminum of 1.4 ev determined by nuclear relaxation measurements and quenching techniques. (4,5)

2.1.1 Simple Theory

The mean energy accepted by a conducting electron when falling through a potential field over its mean free path is

electron volts = El

---

(4) John Cochran and Charles P. Slichter, "Nuclear Relaxation in Aluminum," Physical Review, Vol. 113, No. 6, pp. 1462-1472, March 15, 1959.

(5) R. A. Oriani, "Activation Processes in Solid Metals and Alloys," Edward Arnold Ltd., p. 67, 1964.

(6) Jack Bass, "The Formation and Motion Energies of Vacancies in Aluminum," The Phil magazine, Vol. 15, No. 136, pp. 717, April 1967.

where E is the field intensity and ℓ is the mean free path of the electron.

For typical mean free path lengths on the order of 5×10^{-5} cm the mean energy of the electron at a current density of 10^6 A/cm^2 in aluminum is only 1.3×10^{-4} electron volts.

$$E\ell = \rho J \ell$$
$$= (2.7 \times 10^{-6} \text{ ohm cm})(10^6 \text{ A/cm}^2)(5 \times 10^{-5} \text{cm})$$
$$= 1.3 \times 10^{-4} \text{ eV}$$

This is small compared to the activation energy required for the self-diffusion of aluminum in aluminum of 1.4 $\pm$ 0.1 eV. The electron energy is also small compared to the activation energy for vacancy formation in aluminum of 0.5 to 1 eV.[5,6]

The electron energy picked up by falling through the field is also small compared to the average energy due to thermal agitation at 200°C of 4×10^{-2} eV.

The electric field imposes only a slight drift velocity to the electrons in the metal in the direction of electron flow. This additional energy is not sufficient to lift the metal ions out of the crystalline lattice but can impart upon collision with a thermally activated ion momentum causing ionic drift in the direction of electron flow.

If the net force on the activated ion (total momentum transferred per sec.) directed toward the positive electrode by momentum exchange with electrons exceeds the force on the ion due to the electric field, the aluminum ion will tend to drift toward

the positive electrode. If, however, the force on the ion due to the electric field exceeds that due to electron-ion momentum exchange rate, the ion will tend to drift toward the negative electrode.

If the electrons at zero field are considered to have an entirely random motion, and again a random motion after being accelerated and colliding with ions with nearly elastic collisions (the electron energy picked up from the field and delivered to the ions is small compared to the average thermal energy) the electrons impart all of their momentum to the ions. The rate of reaction which takes place in the migration of aluminum by momentum transfer between thermally activated ions and the electrons should then be a function of the number of activated ions or "targets" available per cm^3, the number of electrons per second available for striking the activated ions and the momentum of these electrons. This may be expressed as:

$$R = F \text{ (electron momentum) (number of electrons striking a unit volume per second) (effective target cross section) (aluminum activated ion density)} \quad (1)$$

where R is the reaction rate and F is a constant.

The additional momentum P picked up by an electron falling through an electric field a distance of its mena-free-path ℓ, with an average velocity v, is

$$P = cE \frac{\ell}{v} = e\rho J \frac{\ell}{v} = eE\tau = e\rho J\tau \quad (2)$$

The average velocity v is determined mainly by the thermal velocity, v_T, and is perturbed only slightly by the drift velocity, v_d. τ is the mean-free-time between collisions, e is the charge on an electron, ρ is the volume resistivity and J the current density.

The arrival rate N of electrons which have been accelerated by the electric field E is related to J by

$$N = nv_d = \frac{J}{e} \tag{3}$$

where n is the electron density.

One may consider the number of activated ions per cubic centimeter in the metal to follow the Arrhenius equation as a function of temperature. Thus,

$$\text{activated aluminum ion density} = F_1 \, e^{-\frac{\phi}{kT}} \tag{4}$$

where ϕ = the activation energy in electron volts
k = Boltzmann's constant 8.62×10^{-5} eV/°K
T = film temperature in degrees Kelvin.

The mean-time-to-failure in hours (MTF) is related to rate of mass transfer by

$$R = \frac{F_2}{MTF} \tag{5}$$

where F_2 is a function of the film geometry.

Equation (1) may be rewritten by substituting Equations (2), (3), (4), and (5) as

$$\frac{F_2}{MTF} = F\left(e\rho J \frac{\ell}{v}\right)\left(\frac{J}{e}\right)(\sigma)\left(F_1 \, e^{-\frac{\phi}{kT}}\right) \tag{6}$$

$$= F\left(\rho \frac{\ell}{v} \sigma J^2\right)\left(F_1 \, e^{-\frac{\phi}{kT}}\right)$$

where σ = ionic scattering cross section. The first term on the right-hand side of this last equation is the force acting between conducting electrons and the ions while the second term expresses

the density of the activated ions as a function of temperature. This equation neglects the opposing force due to the electric field. By consolidation of the constants

$$\frac{1}{MTF} = AJ^2 \exp - \frac{\phi}{kT} \qquad (7)$$

The constant A embodies several physical properites including

(a) the volume resistivity of the metal

(b) the electron free time between collisions or the electron free path and average velocity

(c) the effective ionic scattering cross section for electrons

(d) the frequency factor for self-diffusion of aluminum in aluminum

(e) a film geometric factor relating rate of mass transport with mean-time-to-failure.

Those readers who are interested in further reading on this subject are referred to V. B. Ficks[7] who developed an expression for the force between conducting electrons and ions to be

$$F_{ei} = eE\rho\sigma \qquad (8)$$

In the derivation of this equation the effects of the drift velocity were included into a momentum distribution function and then ignored. Rewriting equation (6) using alternate terms presented in equations (2) and (3) one obtains

---

[7] V. B. Ficks, "On the Mechanism of the Mobility of Ions in Metals," Soviet Physics, Solid State, Vol. 1, No. 1, pp. 14, (1959).

$$\frac{F_2}{MTF} = F\ (eE\ \frac{\ell}{v_t})\ (n\ v_d)\ (\sigma)\ (F_1\ e^{-\frac{\phi}{kT}}) \qquad (9)$$

$$= F\ (eEn\ell\sigma\ \frac{v_d}{v_t})\ (F_1\ e^{-\frac{\phi}{kT}})$$

where the force term differs from equation (8) by the ratio v_d/v_t.

From Equation (7) it would be expected that a plot of $\ln \frac{1}{MTF\ J^2}$ vs $\frac{1}{T°K}$ would be a negative straight line if the factors which contribute to A are slowly varying functions of T. The activation energy derived from the slope of this line would also be expected to be less than 1.4 eV reported for bulk aluminum due to the large surface-to-volume ratio of the films and the generally small crystalline size of condensed aluminum films. The activation energy determined experimentally from the mean-time-to-failure data should serve as a quality figure relating to the degree of perfection of evaporated films.

2.1.2 Small Crystallite Aluminum Films Experiment

An experiment was designed to determine the values of ϕ and A for highly polycrystalline aluminum films. These were deposited in a high vacuum at the low 10^{-8} Torr pressure range by the evaporation of 99.999 percent aluminum from tungsten filaments on a cold (<100°C) substrate. The crystallite lateral size was about 1.2 microns. The substrate consists of 9000 Å of SiO_2 on silicon wafers. The films were etched to form conductor paths 54 x 0.5 mil x 7000 Å, and brazed into TO-5 headers. These were wire-bonded using 0.001-inch diameter aluminum wire, and a can was welded to the header encapsulating the film in a dry nitrogen ambient. Each cell consisted of 10 devices from which the mean-time-to-failure was determined. The current density varied from 0.5 to 2.88 x 10^6 A/cm^2 and the mean-time-to-failure ranged from 1.5 to 850 hours.

Table I presents the experimental failure data obtained for these films.

TABLE I

TEST DATA FOR SMALL CRYSTALLITE ALUMINUM FILMS

Film No.	Thickness (Å)	Width (mils)	$J \times 10^{-6}$ (A/cm^2)	T (°C)	$\frac{10^3}{T°K}$	MTF (Hours)	$\frac{10^{14}}{MTF\ J^2}$
AD	7400	0.56	0.5	177	2.22	480	0.83
BD	7060	0.50	1.21	186	2.18	47	1.45
CD	7000	0.50	1.5	195	2.135	19.5	2.28
DD	6800	0.56	2.82	238	1.96	3.5	3.70
AB	7400	0.56	0.5	192	2.15	250	1.60
BB	7060	0.50	1.22	200	2.11	38	1.80
CB	7000	0.50	1.5	212	2.06	8	5.55
DB	6800	0.56	2.88	260	1.87	1.5	8.03
BA	7060	0.50	0.987	109	2.62	850	0.121
CA	7000	0.50	1.46	121	2.54	268	0.175
DA	6800	0.56	2.05	134	2.48	183	0.130

The film temperature was determined by the oven temperature plus the rise in temperature due to film power dissipation. For the TO-5 header, a thermal impedance of 190°C per watt was employed.

A plot of

$$\ln \frac{1}{MTF\ J^2} \text{ vs } \frac{1}{°K}$$

is presented in Figure 3. Except for two maverick points where the raw data on failure rate was difficult to evaluate, a straight line fits the data quite well. For these data the current density varied

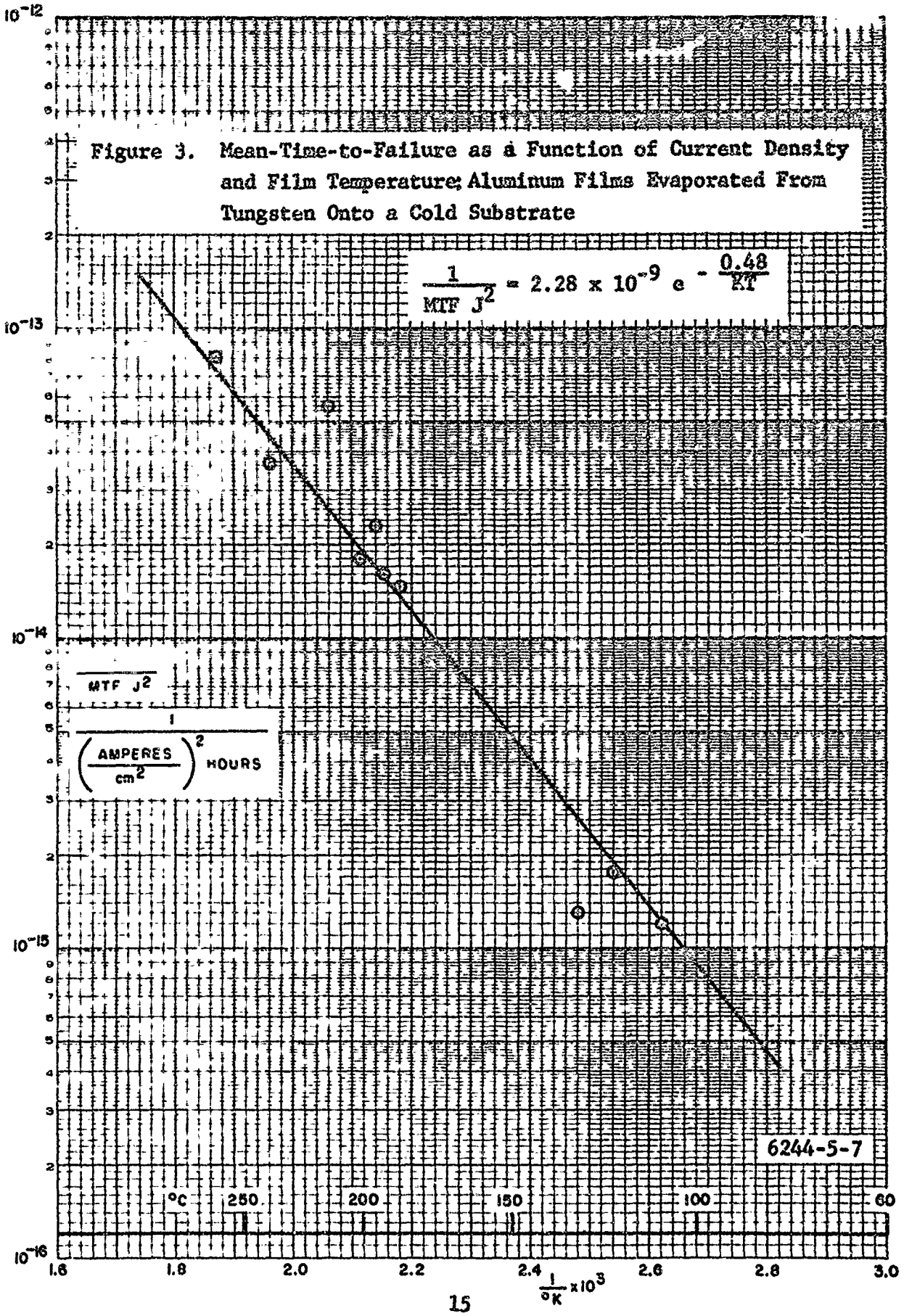

Figure 3. Mean-Time-to-Failure as a Function of Current Density and Film Temperature; Aluminum Films Evaporated From Tungsten Onto a Cold Substrate

greater than 5 to 1 while the temperature varied 1.4 to 1 on the Kelvin scale. The equation representing this line is

$$\frac{1}{MTF\ J^2} = 2.28 \times 10^{-9}\ e^{-(0.48/kT)} \qquad (10)$$

The activation energy of 0.48 eV is 34 percent of that reported for the self-diffusion of aluminum in aluminum of 1.4 eV.

2.1.3 Large Crystallite Aluminum Film Experiment

Data has been gathered on the life of well ordered aluminum film conductors containing large crystallites. The films were deposited from tungsten filaments in the low 10^{-8} Torr region using aluminum source material which was 99.999 percent pure. The large crystallites (approximately 8 microns lateral geometry) were obtained by maintaining the substrate temperature at 400°C during the deposition. The film thickness was 6000 Å and the line width was in excess of 0.6 mils. The cells were stressed at current densities ranging from 0.55 to 2.02×10^6 A/cm^2 and the mean-time-to-failures ranged from 12 to 1125 hours. The data for this film structure is presented in Table II and plotted in Figure 4. The formula relating current density and temperature to mean-time-to-failure is

$$\frac{1}{J^2\ MTF} = 5.18 \times 10^{-6}\ e^{-(0.84/kT)} \qquad (11)$$

The increase in activation energy to 0.84 eV for this failure mode for the large crystallite well ordered films over the activation energy of fine grained aluminum films is attributed to the reduction of grain boundaries with their associated high self-diffusion coefficient.

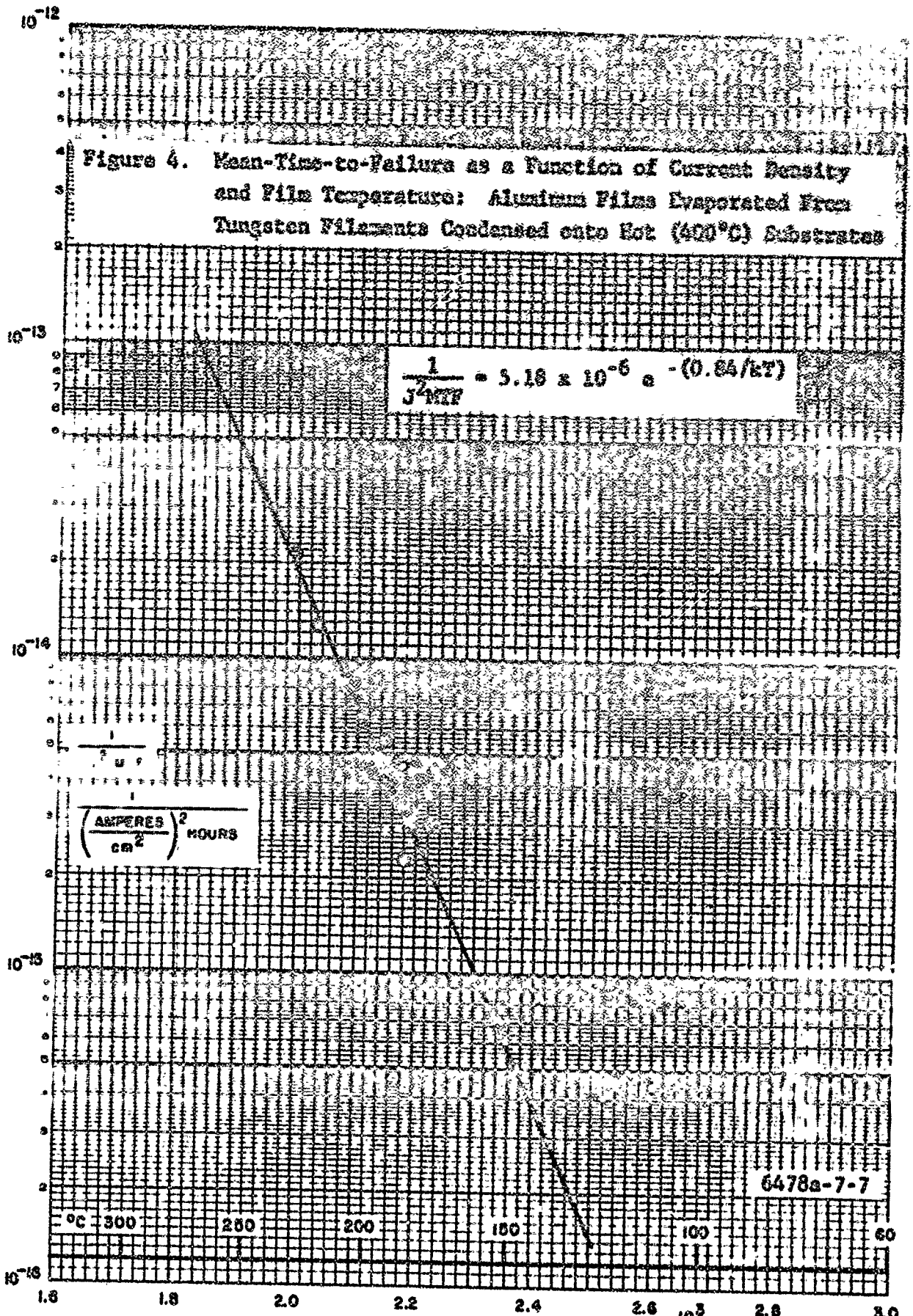

Figure 4. Mean-Time-to-Failure as a Function of Current Density and Film Temperature: Aluminum Films Evaporated From Tungsten Filaments Condensed onto Hot (400°C) Substrates

TABLE II

TEST DATA FOR LARGE CRYSTAL ALUMINUM FILMS

Film No.	Thickness Å	Width (mils)	$J \times 10^{-6}$ (A/cm^2)	MTF (Hours)	$\frac{10^{15}}{J^2 MTF}$	T (°C)	$\frac{10^3}{T°K}$
AB	6036	0.582	0.6	510	5.45	193	2.145
EB	6036	0.644	1.27	270	2.30	183	2.18
CB	6036	0.644	1.106	254	3.22	185	2.18
DB	6036	0.638	1.95	20.3	12.9	220	2.03
BB	6036	0.644	1.15	180	4.21	205	2.09
CB	6036	0.644	1.37	63	8.45	206	2.085
DB	6036	0.638	1.97	12	21.6	230	1.99
AD	6036	0.582	0.548	1125	2.96	177	2.22
DA	6036	0.638	2.02	53	4.63	184	2.19
CA	6036	0.644	1.31	840	0.695	155	2.34

2.1.4 Large Crystallite Aluminum Films With a Glass Film Overcoat

A further increase in activation energy for mass transport should be obtained by the elimination of surface diffusion which is a dominating factor for thin films possessing a high surface-to-volume ratio. By the reduction of both grain boundary and surface diffusion it was predicted that the activation energy should approach that for self-diffusion of aluminum through the crystal lattice of 1.4 eV.

Large crystallite aluminum films were prepared with an overcoat of silica glass deposited by the vapor plating technique to a thickness of 7,000 Å in an attempt to reduce surface diffusion. These aluminum films were 12,200 Å thick and possessed a width of

1.46 mils. The current density for the cells varied from 0.46 to 0.908 x 10^6 A/cm^2 and the mean-time-to-failure ranged from 395 to a predicted 16,000 hours. This experiment was terminated with three of the six cells exhibiting greater than 50 percent failures (3900 hours)

Tables III and IV present the data for the failed films and the predicted lifetime based upon Poisson's distribution of those films which have been aged but have not reached the 50 percent failure time.

TABLE III

GLASSED LARGE CRYSTAL ALUMINUM PERFORMANCE

Film Thickness Å	Film Width (mils)	$Jx10^{-6}$ A/cm^2	MTF Hours	$\frac{10^{15}}{J^2 MTF}$	Film Temp.	$\frac{10^3}{°K}$
12,200	1.46	0.908	1700	0.713	212	2.06
12,200	1.46	0.860	1060	1.28	221	2.02
12,200	1.43	0.870	395	3.33	246	1.93

TABLE IV

GLASSED LARGE CRYSTAL ALUMINUM PREDICTED PERFORMANCE

Film Thickness (Å)	Film Width (mils)	$Jx10^{-6}$ (A/cm^2p)	Estimated MTF Hours	$\frac{10^{15}}{J^2 MTF}$	Film Temp. °C	$\frac{10^3}{°K}$	Sample Size	No. of Failures	Hours on Test
12,200	1.46	0.777	5,400	0.306	203	2.10	15	7	3900
12,200	1.46	0.702	12,000	0.170	189	2.16	13	2	2590
12,200	1.46	0.460	16,000	0.295	200	2.11	13	1	2333

Figure 5 presents this data. The formula relating current density and film temperature to the mean-time-to-failure for well ordered glassed aluminum films is

$$\frac{1}{J^2 MTF} = 1.88 \times 10^{-3} e^{-(1.2/kT)} \qquad (12)$$

The activation energy of 1.2 eV for these thick, wide, well ordered and glassed films approaches the predicted maximum activation energy of 1.4 eV which is the activation energy for self-diffusion of aluminum in bulk aluminum. The increase in activation energy for these films over well ordered nonglassed films reported on in the previous section is attributed to the reduction in surface diffusion due to the overlaying glass film Also, because of its increased thickness, these films are probably better ordered than were the thinner nonglassed films, tending to enhance the activation energy.

2.1.5 Aluminum Film Lifetime as a Function of Conductor Stripe Cross-Sectional Area

The simple theory, as presented in Equation 7 of section 2.1, expressed the relationship between the mean-time-to-failure of a group of conductors to current density, temperature and the degree of order of the deposited film. The activation energy ϕ varies with the degree of film crystalline order ranging from near 0.5 eV for highly polycrystalline films to a theoretical maximum of 1.4 eV for well-ordered large-grained bulk aluminum.

The preexponential constant "A" was shown to contain a factor which relates the lifetime of the film to the cross-sectional area of the conductor stripe. Since for a given rate of transport or void growth, the greater the film cross-sectional area, the longer it should take to cause a void to grow across the conductor resulting in an open circuit.

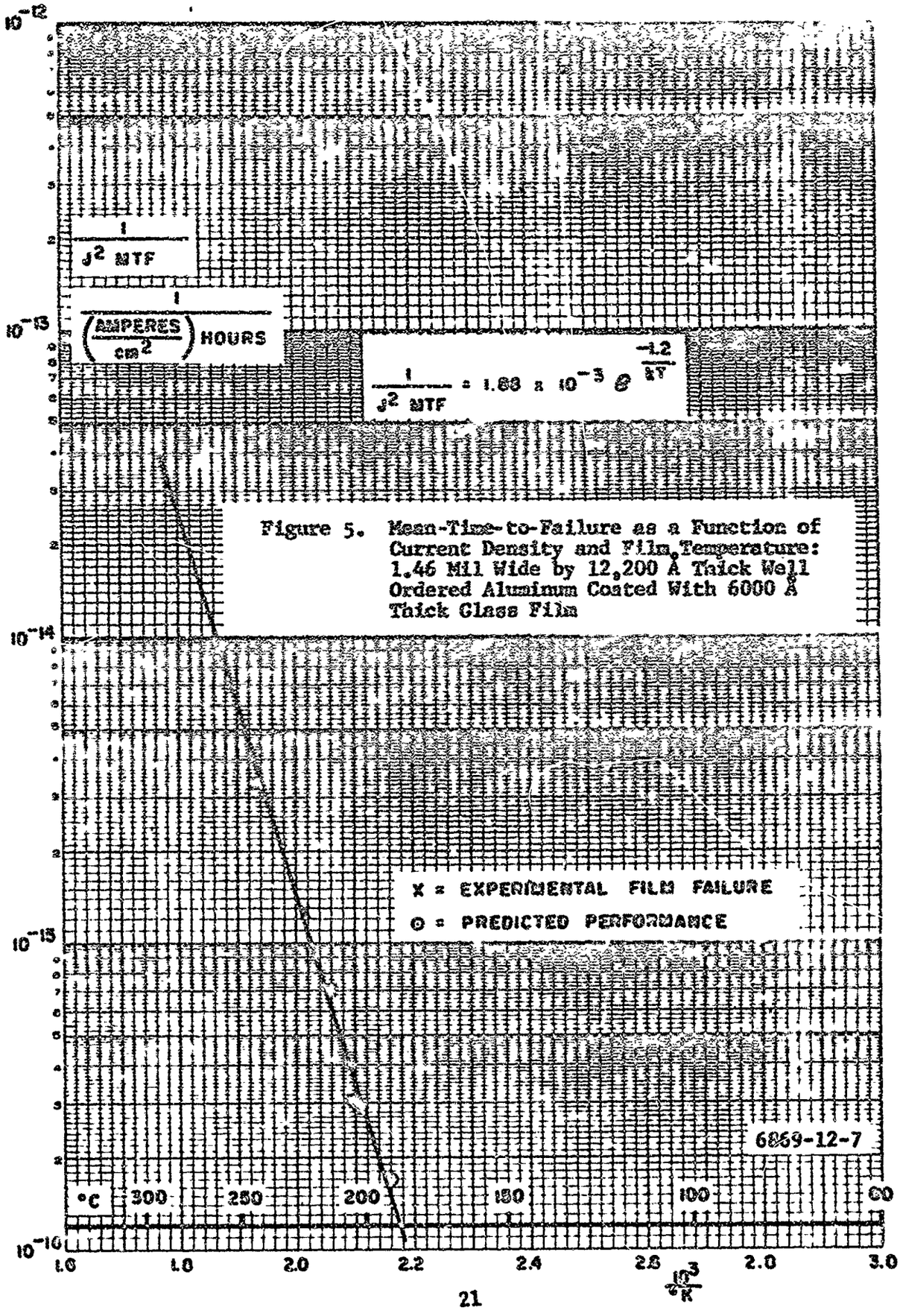

Figure 5. Mean-Time-to-Failure as a Function of Current Density and Film Temperature: 1.46 Mil Wide by 12,200 Å Thick Well Ordered Aluminum Coated With 6000 Å Thick Glass Film

To include the effect of line geometry in the above equation, two life test experiments were initiated. In the first experiment the line thickness was maintained near 7000 Å but the line width was caused to vary from 0.45 to 1.98 mils. For the second experiment the line width was maintained constant at 0.5 mil while conductor stripe thickness was varied from 1,921 Å to 12,540 Å. Aluminum, 99.999 percent pure, was evaporated from tungsten filaments at the low 10^{-8} Torr pressure onto oxidized silicon substrates heated to 420°C. Large-grained well-ordered crystallites were formed by this process. Conductor stripes were then etched into these films which were then placed under current density and temperature stress.

Table V presents the data obtained on devices of variable line widths with 11 different cells which were placed under lifetime test at elevated current density and temperature stress. The last column in the table lists the calculated mean-time-to-failure utilizing the formula presented in Equation 11 of section 2.1.3 for the lifetime of nonglassed large-grained aluminum films normalized to the cross-sectional area of those films. Equation 11 was derived for 6036 Å thick films possessing an average line width of 0.63 mil. The pre-exponential constant, when normalized to the average cross-sectional area of the film (9.65×10^{-8} cm^2), becomes

$$5.18 \times 10^{-6} \times 9.65 \times 10^{-8} = 5 \times 10^{-13} \qquad (13)$$

The resultant new formula which accounts for the conductor cross-sectional area is therefore:

$$\frac{1}{J^2 MTF} = \frac{5 \times 10^{-13}}{B} \exp\ (-0.84/kT) \qquad (14)$$

where B is the conductor cross-sectional area expressed as cm^2.

TABLE V

TEST DATA FOR LARGE CRYSTAL ALUMINUM FILM CONDUCTORS OF VARIABLE LINE WIDTHS

Film Thickness (Å)	Film Width (mils)	Film Cross-sectional Area ($cm^2 \times 10^8$)	$J \times 10^{-6}$ (A/cm^2)	T (°C)	$\frac{10^3}{T(°K)}$	Experimental MTF (hours)	Calculated MTF (hours)
7540	0.45	8.62	1.85	167	2.275	230	211
7540	0.94	18.0	1.42	170	2.26	650	660
7540	1.40	26.8	1.48	190	2.16	320	341
7540	1.87	35.9	1.51	230	1.98	76	76
7265	0.46	8.42	1.48	205	2.09	96	76
7265	0.93	17.1	1.42	219	2.035	47	69
7265	1.42	26.2	1.39	231	1.985	49	68
7125	0.54	9.75	1.51	196	2.135	130	93
7125	1.00	18.1	1.57	210	2.07	127	84
7125	1.47	26.6	0.93	198	2.12	670	575
7125	1.98	36.8	1.00	210	2.07	450	420

The formula for large-grained aluminum can be rewritten to be:

$$MTF = \frac{(w)(t)\ \exp\ (0.84/kT)}{5 \times 10^{-13}\ J^2} \qquad (15)$$

where MTF = mean-time-to-failure in hours

w = conductor width in cm

t = conductor thickness in cm

k = Boltzmann's constant (8.62×10^{-5} eV/atom/°K)

J = current density in amperes per square centimeter

T = absolute temperature of the conductor

A graphical presentation of the experimental vs the calculated mean-time-to-failure for these data is shown in Figure 6. From this it appears that mean-time-to-failure varies in a linear manner with the line width of the conductor stripe.

In the second portion of this investigation, aluminum conductor stripes were prepared and placed under stress tests to evaluate the effect of conductor thickness. Well ordered aluminum films possessing a line width of about 0.5 mil and thicknesses varying from 2,000 to 12,000 angstroms were tested. Data for this test is presented in Table VI. The formula utilized to calculate the mean-time-to-failure presented in this table was that of Equation (15). A plot of the experimental vs the calculated mean-time-to-failure for these films is given in Figure 7. Unfortunately, due to lack of time, the stress conditions for this experiment were chosen to obtain rapid failures which tends to increase errors and introduce a greater spread in the data than that obtained at low stress conditions. (This is observed in Figure 6.) It is concluded, however, from Figures 6 and 7 that the film lifetime is a function of the film cross-sectional area and that Equation 15 is a valid expression relating mean life to the film geometry, film temperature and current density for well ordered films.

Figure 8 presents a graph relating the experimentally determined film volume resistivities as a function of film thickness. (The two points at 4790 and 5440 angstroms were obtained from films which were constructed but not placed under stress test because they were similar to those already discussed in Section 2.1.3.)

It is seen that for film thicknesses below 5,000 angstroms the volume resistivity rapidly increases. This is attributed to the fact that the mean-free-path of electrons in aluminum at these temperatures is about 5,000 angstroms and electron collisions at the

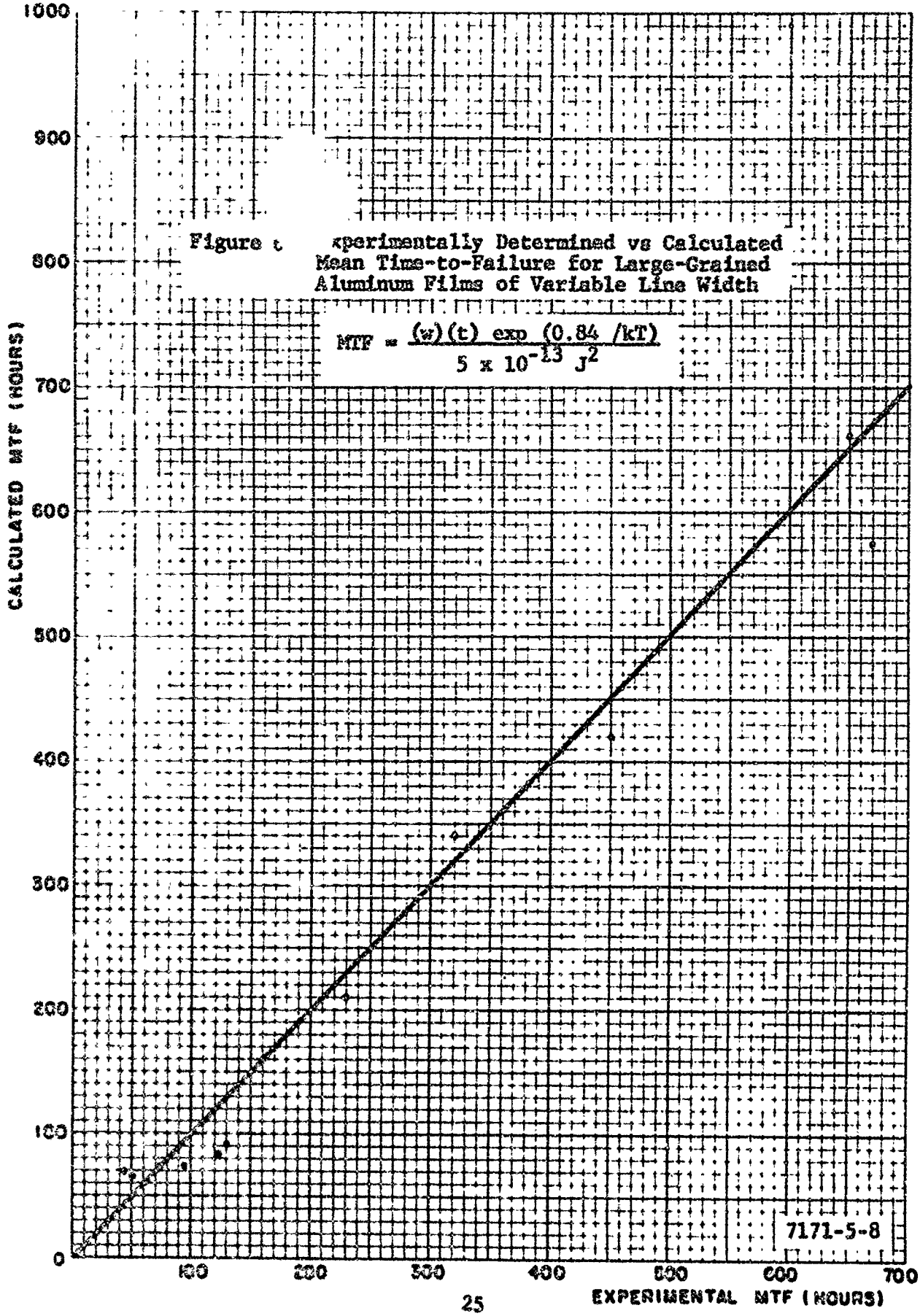

Figure t xperimentally Determined vs Calculated Mean Time-to-Failure for Large-Grained Aluminum Films of Variable Line Width

$$MTF = \frac{(w)(t)\ \exp\ (0.84\ /kT)}{5 \times 10^{-13}\ J^2}$$

TABLE VI

TEST DATA FOR LARGE CRYSTAL ALUMINUM FILM CONDUCTORS OF VARIABLE THICKNESS

Film Thickness (Å)	Film Width mils	Film Cross-sectional Area ($Cm^2 \times 10^6$)	$J \times 10^{-6}$ (A/cm^2)	T (°C)	$\frac{10^3}{T(°K)}$	Experimental MTF	Calculated MTF	Volume Resistivity ohm-cm $\times 10^6$
2017	.63	3.22	2.010	204	2.100	24	21	6.02
2088	.66	3.48	1.780	204	2.10	35	16	7.05
2460	.57	3.53	2.07	200	2.115	36	14	4.82
3320	.52	4.38	1.560	192	2.15	33	45	3.53
3840	.58	5.66	2.175	206	2.09	11	17	3.42
8838	.51	11.42	1.477	202	2.10	80	80	3.05
9455	.43	10.32	1.457	200	2.115	62	86	3.06
10500	.39	10.40	1.460	200	2.115	100	87	3.04
12540	.42	13.38	1.655	222	2.02	38	35	3.11

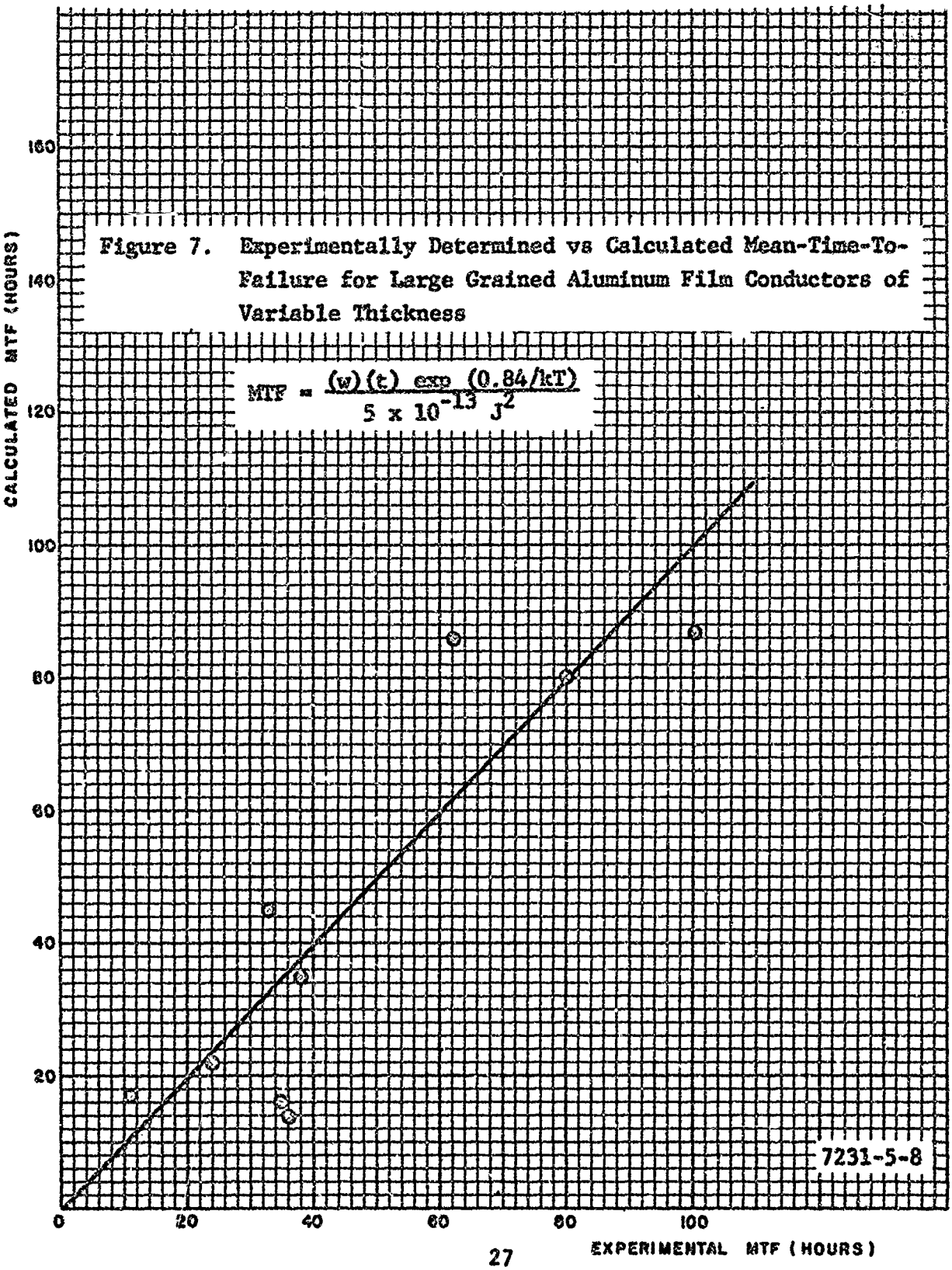

Figure 7. Experimentally Determined vs Calculated Mean-Time-To-Failure for Large Grained Aluminum Film Conductors of Variable Thickness

Figure 8. Al Film Resistivity Normalized to Bulk Resistivity as a Function of Film Thickness

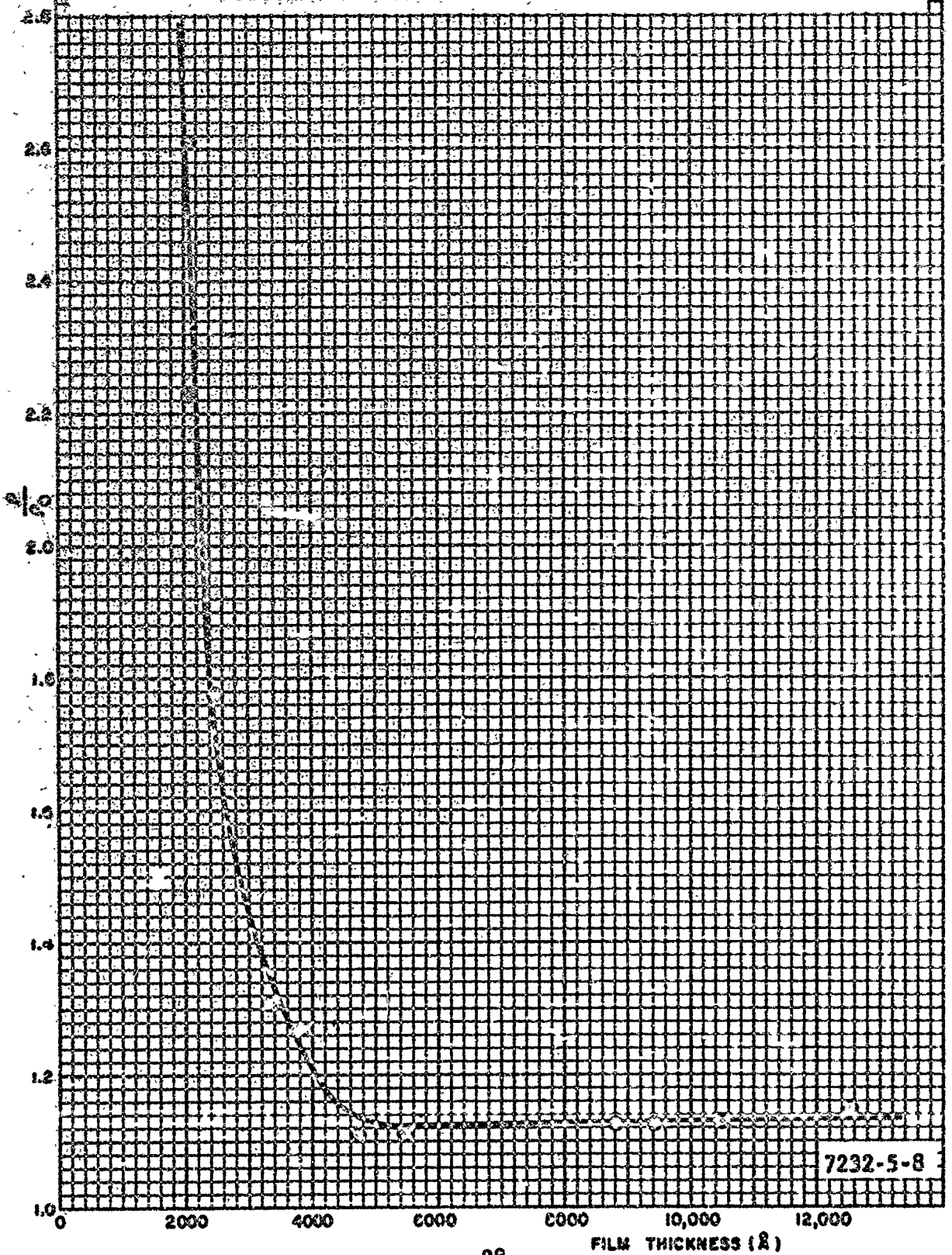

conductor boundary become important in determining the resistivity for film thicknesses less than the electron mean-free-paths. This fore-shortening of the electron mean-free-path, however, does not affect the rate of mass transport of the aluminum. The Sommerfield theory indicates that ρ and ℓ are inversely related to one another.[8] Thus, by inspection of the momentum formula presented in Equation (2) it is seen that as ℓ decreases, and ρ increases, the momentum picked up by the electron remains constant for a given metal at a given current density.

2.1.6 Summary of the Mass Transport of Aluminum by Momentum Exchange with Conducting Electrons in the Absence of Material Gradients, Temperature Gradients or Current Density Gradients

In the proceeding sections a simple theory has been generated and experiments described to illucidate the transport of aluminum ions in aluminum film conductors under current density and temperature stress. In this section this information is summarized and presented in a fashion useful to device design engineers.

An equation based upon simple theory was derived in Section 2.1.1 Equation (7), relating the mean-time-to-failure for aluminum film conductors to current density, temperature, an activation energy and a constant embodying several physical properties. The activation energy has been experimentally determined to be a function of the degree of order of the aluminum film varying from 0.5 eV for fine grained films to 0.8 eV for well ordered films and to 1.2 eV for well ordered glassed aluminum films. (Sections 2.1.2, 2.1.3, and 2.1.4.) It was also determined in Section 2.1.5 that the value for the preexponential constant in Equation (7) varied in a linear manner with the conductor film cross-sectional area.

---

(8) E. H. Sondheimer, "The Mean Free Path of Electrons in Metals," Advances in Physics, Vol.1, No. 1. Jan. 1952.

Normalizing the data for the experiments described in Sections 2.1.2, 2.1.3, and 2.1.4 to account for the film cross-sectional area, only the preexponential constants are changed to give the resulting formulas:

Small Crystallite Films (α 1.2 μ)

$$\frac{MTF}{J^2 MTF} = 2.43 \times 10^{-16} \exp - (0.48/kT) \qquad (16)$$

Large Crystallite Films (α 8μ)

$$\frac{MTF}{J^2 MTF} = 5 \times 10^{-13} \exp -(0.84/kT) \qquad (17)$$

and Large Crystallite Glassed Films

$$\frac{MTF}{J^2 MTF} = 0.5 \times 10^{-10} \exp -(1.2/kT) \qquad (18)$$

where w and t are the conductor width and thickness expressed in centimeters.

Figure 9 presents these equations as an Arrhenius plot. As shown, these intersect at a temperature near 275°C. At this temperature and above, lattice diffusion effects are predominant over surface and grain boundary diffusion; thus structural effects are not important in that temperature range. At temperatures lower than 275°C, however, orders of magnitude improvement in lifetime can be obtained through the use of well ordered large-grained films and well-ordered large-grained glassed films.

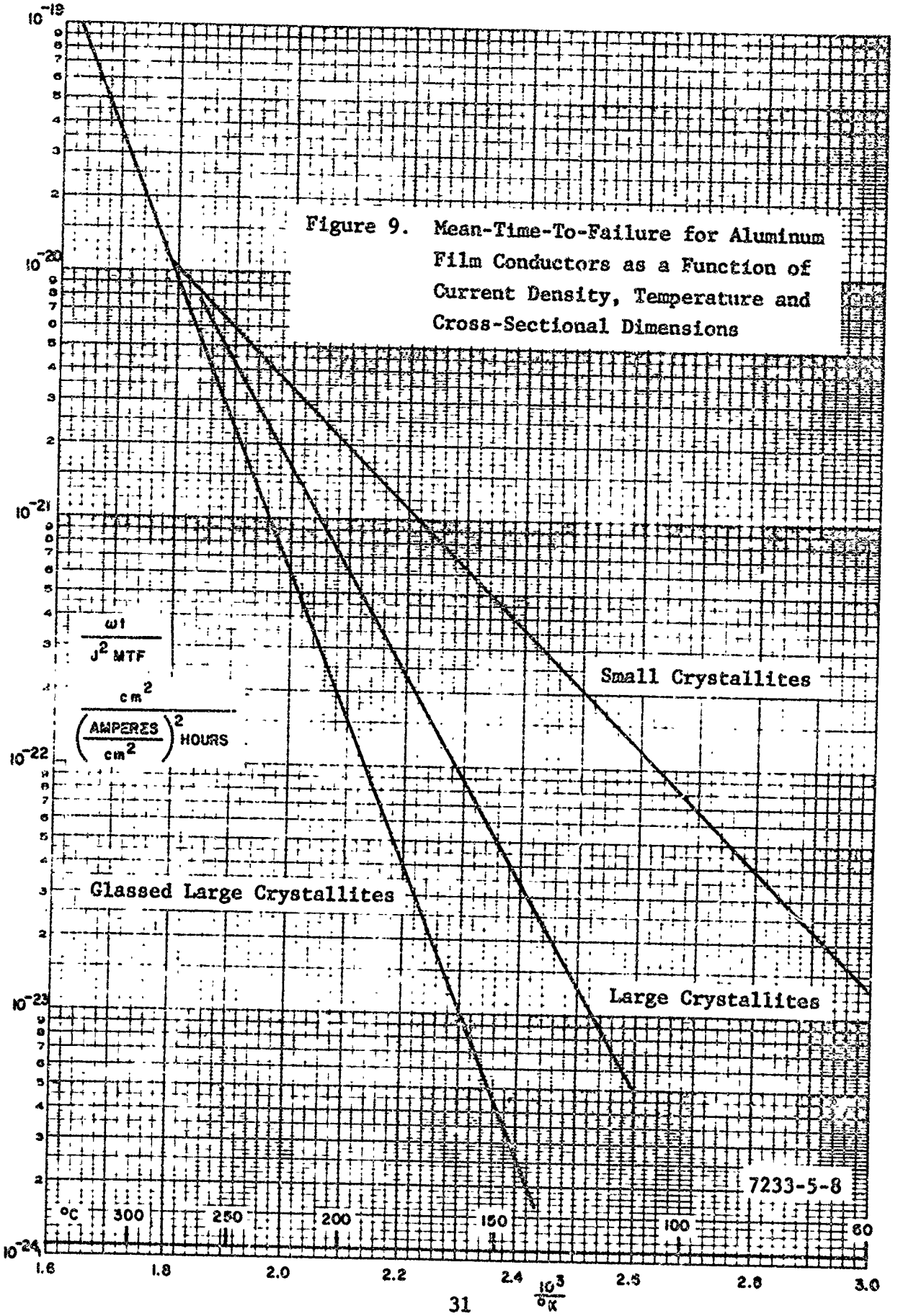

Figure 9. Mean-Time-To-Failure for Aluminum Film Conductors as a Function of Current Density, Temperature and Cross-Sectional Dimensions

An alternate form for Equations (16), (17), and (18) useful in design work is given below.

Small Crystal Films (1.2 microns)

$$MTF = \frac{w\ t\ \exp\ (0.48/kT)}{2.43 \times 10^{-15}\ J^2} \qquad (19)$$

Large Crystal Films (8 microns)

$$MTF = \frac{w\ t\ \exp\ (0.84/kT)}{5 \times 10^{-13}\ J^2} \qquad (20)$$

Large Crystallite Glassed Films

$$MTF = \frac{w\ t\ \exp\ (1.2/kT)}{8.5 \times 10^{-10}\ J^2} \qquad (21)$$

These equations are plotted in Figures 10, 11, and 12 using the product w t to be 10^{-7} cm^2. This value is equal to a 0.5 mil by 7,200 Å thick film and is typical of conductor stripes for integrated circuits. Since the lifetime is directly proportional to the film cross-sectional area, the life of films possessing other cross sections can be quickly determined from these plots.

2.2 MASS TRANSPORT OF ALUMINUM AT ALUMINUM-SILICON CONTACTS

In Section 2.1 the failure of aluminum conductors stressed at high current densities and temperatures was discussed when the conductor experienced no temperature, current density or compositional gradients. In general, accelerated failure rates are anticipated in conductors which contain a compositional, a thermal or a current density gradient. The failure mode is a void which rapidly grows

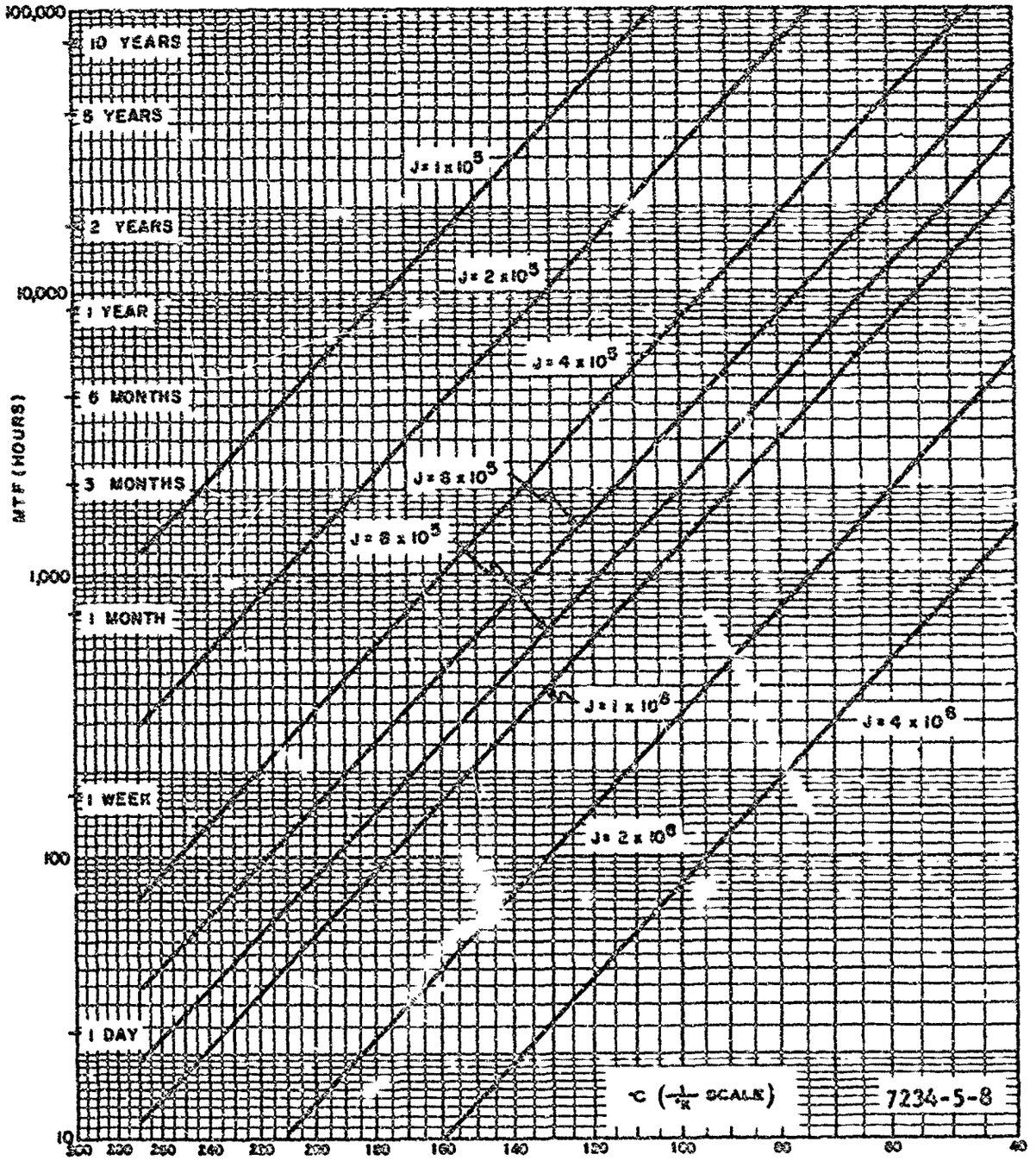

Figure 10. Small Crystallite Aluminum Film Lifetime of Conductors With 10^{-7} cm^2 Cross-Sectional Ar

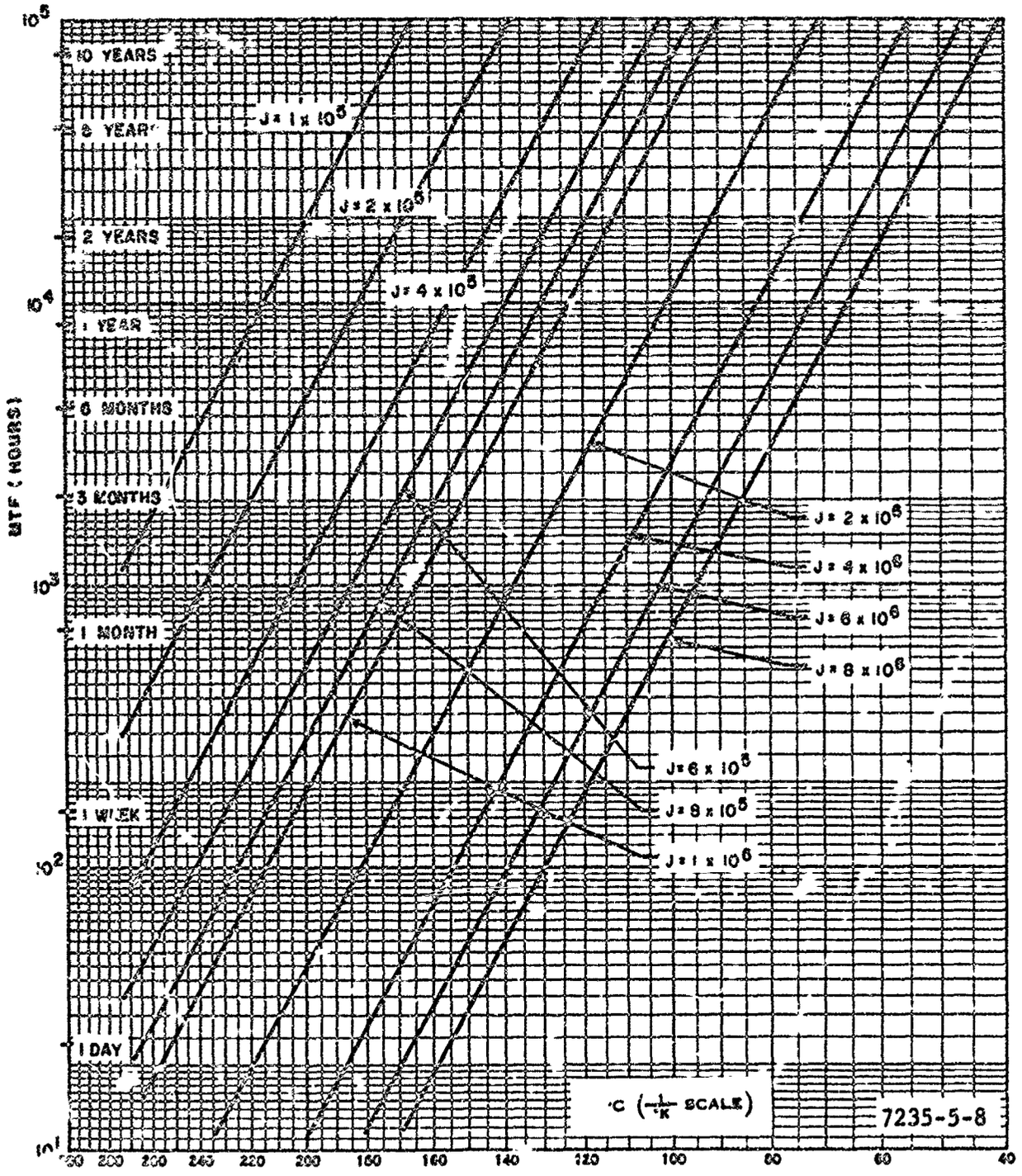

Figure 11. Large Crystallite Aluminum Film Lifetime of Conductors With 10^{-7} cm^2 Cross-Sectional Area

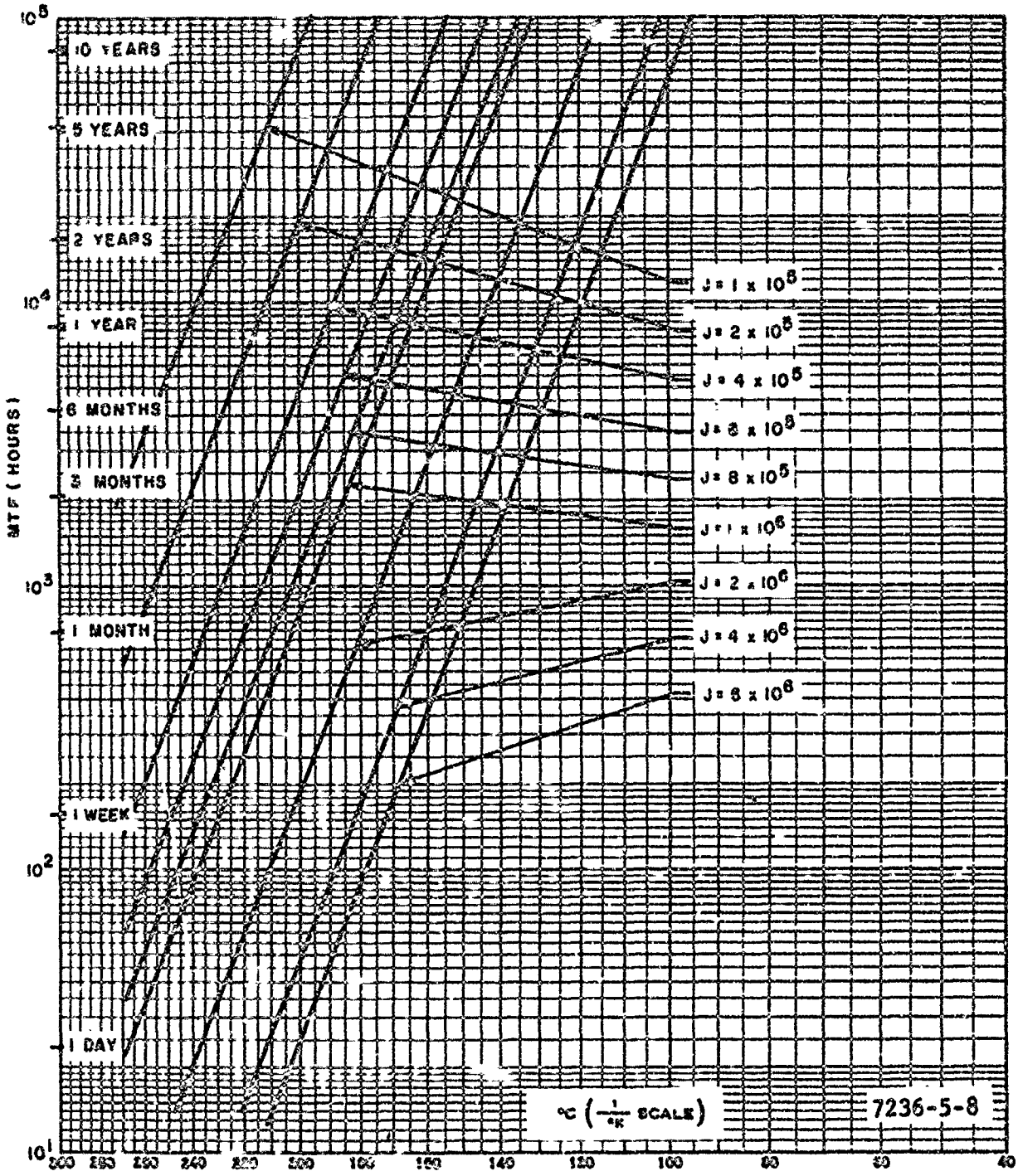

Figure 12. Glassed Large Crystallite Aluminum Film Lifetime for Conductors with a Cross-Section of 10^{-7} cm^2

across the aluminum film downstream (in terms of electron flow) from a positive thermal, positive current density or positive diffusion coefficient gradient. (The sign of the gradient is taken to be positive when the quantity increases in the direction of electron flow; see Figure 13.) Vacancies, which migrate toward the negative end of the conductor, cluster at these regions to form voids. The clustering is accelerated due to the reduced mobility of the vacancies when entering regions of lower temperature, lower current density or of lower diffusion coefficient.

For similar reasons whiskers and hillocks of aluminum grow upstream (in terms of electron flow) from negative thermal, negative current density or negative diffusion coefficient gradients. In these regions aluminum ions which migrate in the direction of electron flow are caused to cluster at certain crystalline defects and crystallite sites to form whiskers and nondescript extruded-appearing mounds of aluminum. Clustering upstream from a gradient is caused by the reduction in ionic mobility due to the negative thermal gradient, the negative current density gradient or a negative diffusion coefficient gradient. The diffusion coefficient gradient may result from a compositional gradient.

To qualitatively study the effect that a compositional gradient has on the failure of aluminum conductors, diffused silicon resistors contacted by aluminum were stressed at elevated temperatures and current densities.

Figures 14a and 14b present photomicrographs (600X) of two sets of three diffused resistors contacted by aluminum and aged at 235°C at an aluminum stripe current density of 1.3×10^5 A/cm^2. The three contacts near the center of the figures are the negative

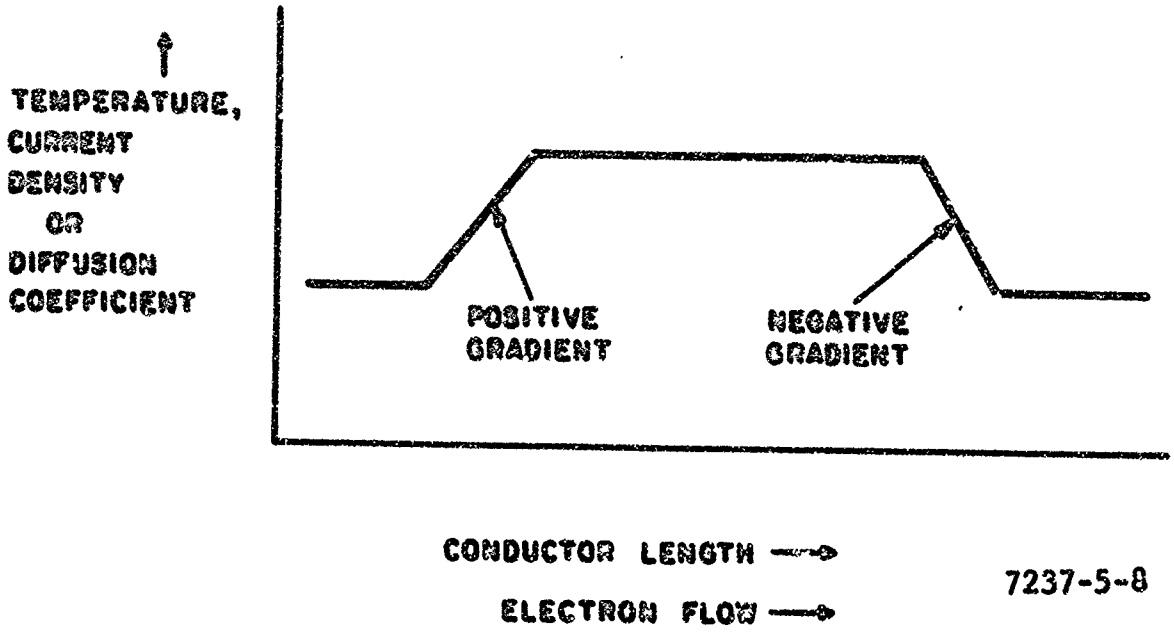

Figure 13. Definition of Gradients

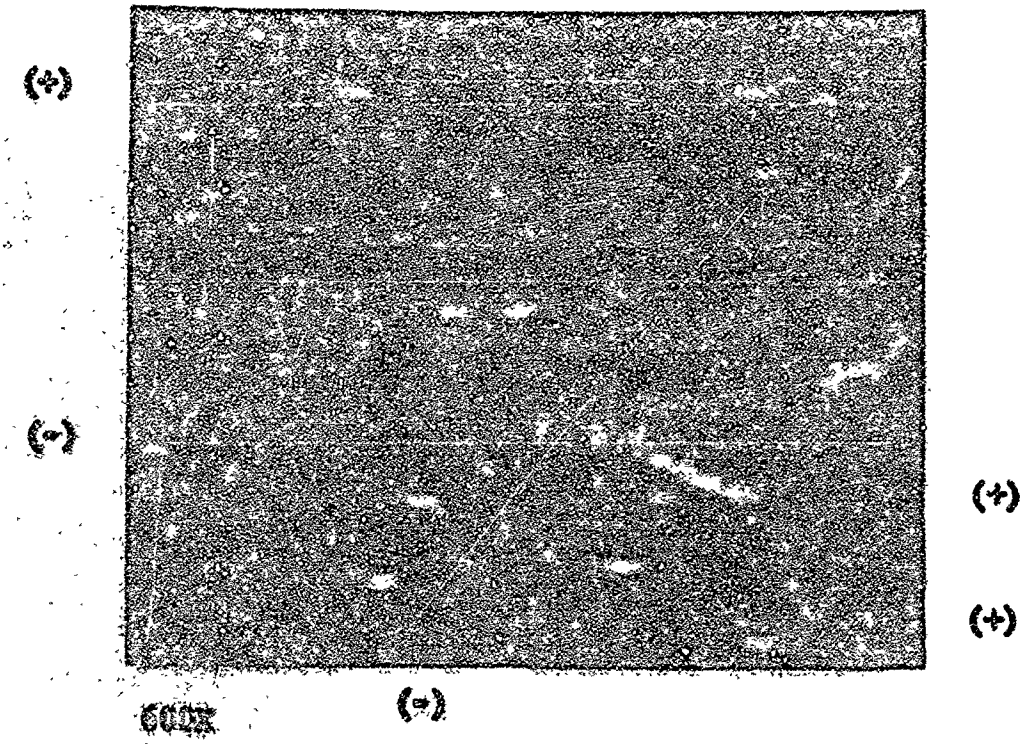

(a)

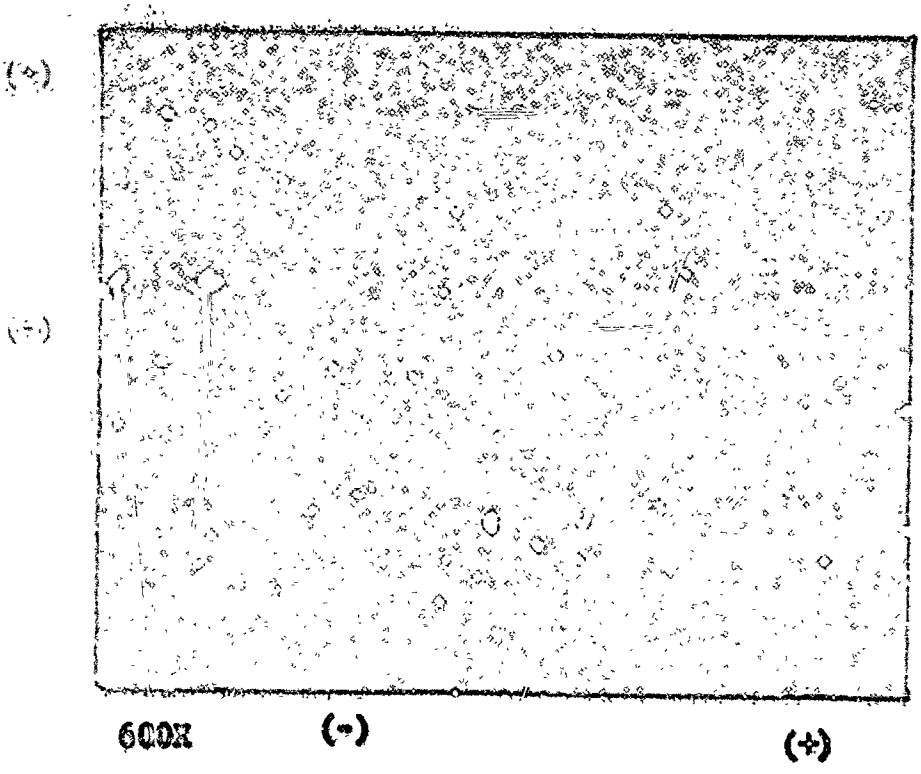

(b)

Figure 14. Al Contacts to Si Diffused Resistors After Aging at $J = 1.3 \times 10^5$ A/cm^2 at 235°C for 230 Hours

terminals and all exhibit aluminum whisker and nodule growth at the silicon-aluminum contacts. This is explained by the transport of aluminum ions to these contacts by momentum exchange between thermally activated ions and conducting electrons. At the silicon-aluminum interface the aluminum ions accumulate to form nodules and whiskers since they are prevented from traveling further by the silicon with its low solid solubility for aluminum.

The failure mode appears only at the positive terminals where it is seen from the photomicrographs of Figure 14 that a degradation of the aluminum has occurred as observed by a darkening of the aluminum and voids extending across some of the conductor stripes resulting in open circuits. Aluminum is transported away from the contact area by momentum exchange with conducting electrons. Since at this interface there are no further aluminum ions available upstream (from the silicon) to fill in vacancies created by the departing aluminum ions, the vacancies rapidly cluster to form a void which eventually grows across the stripe, resulting in an open circuit.

A second set of diffused resistors contacted by aluminum films were aged at 236°C at an aluminum stripe current density of 1.3×10^5 A/cm^2. The polarity of these samples were reversed from those discussed above. As seen in Figure 15a and 15b, hillocks and whiskers of aluminum grow near the negative terminals while voids and depletion of the aluminum occur near the positive contacts to the diffused silicon resistors. By comparison with Figure 14, it is seen that the formation of hillocks or voids at the contacts is determined by the direction of electron flow. This also serves as a further proof that the transport of aluminum is in the direction of electron flow.

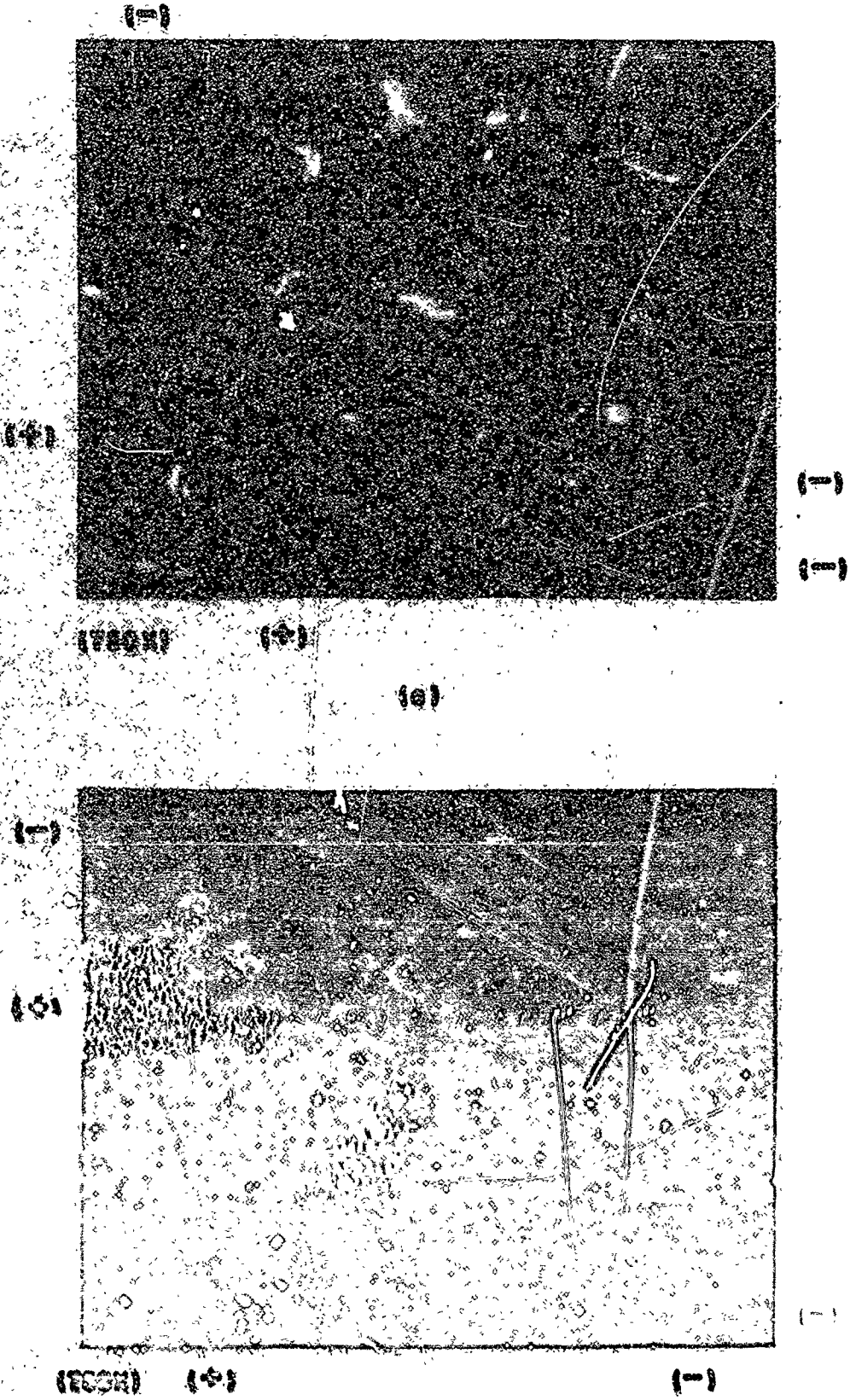

Figure 15. Aluminum Contacts to Silicon Diffused Resistors After Aging at $J = 1.3 \times 10^5$ A/cm^2 and 235°C for 250 Hours

Another effect of aluminum metal transport was observed in this investigation. The aluminum bonding wires were removed from the samples to enable the use of high magnification objective lenses during their inspection. One of the negative bonding wires was apparently attached to the aluminum film bonding pad only over a small contact area. The current density in the film at the periphery of this small contact was sufficiently high to cause a depletion of the aluminum in the film. The photomicrograph of Figure 16 shows the depletion of the aluminum film under the bonding pad as a darkened region. This is an excellent example of void growth at a current density gradient.

Three diffused silicon resistors contacted by aluminum plus 3-percent silicon conductors were aged for 140 hours at an aluminum current density of 1.3×10^5 A/cm^2 and 235°C. The samples were similar to those described in the above paragraphs and contain steep built-in compositional gradients at the silicon-aluminum interfaces. An optical micrograph of the diffused resistors is presented in Figure 17. Whiskers and hillocks of aluminum grow at the negative terminals to the silicon while depletion of the aluminum takes place near the positive contacts to silicon.

Scanning electron micrographs were made of this sample. Figure 18 shows the region near contact No. 1 of resistor No. 1 as identified in the previous figure. Hillocks grow near this negative contact and one whisker 0.066 mil in diameter is observed.

Figure 19 is a view of the positive contacts No. 2 and No. 3 to resistors 1 and 2. The holes through the glass layer enabling contact to be made to these resistors are 0.50 x 0.33 mil. Severe depletion of the aluminum from the glass surface near these contacts is observed as a darkened region.

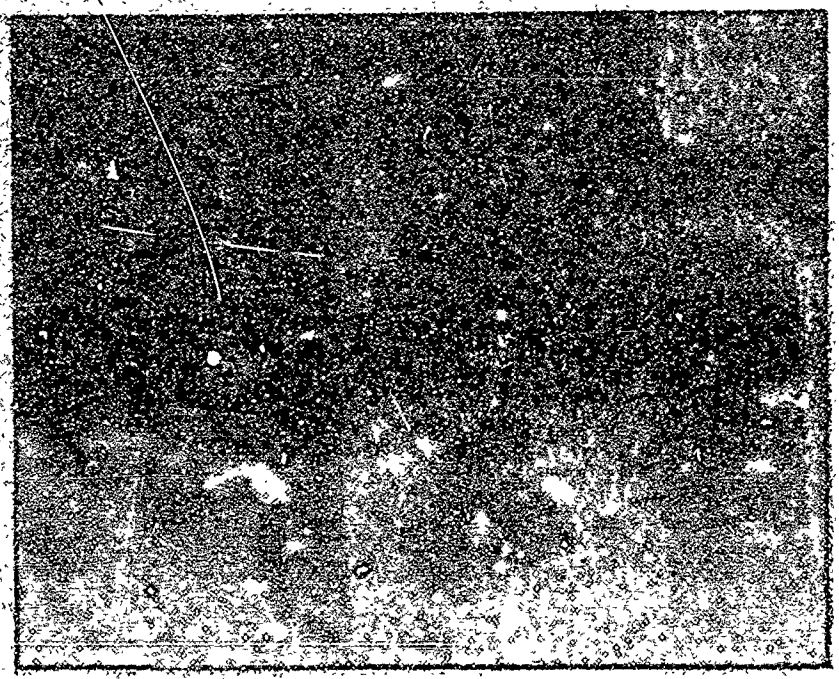

(750 X)

(−)

(−)

Figure 16. Depletion of Al Under a Wire Bond Which Made a Small Area Contact to the Film

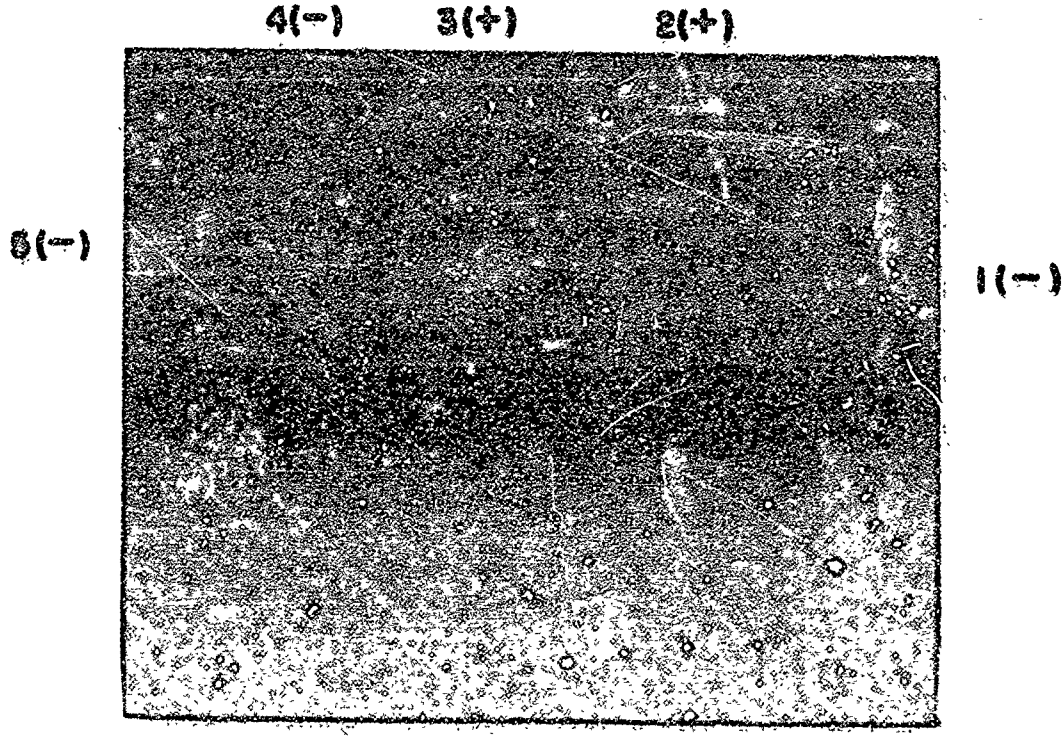

RESISTOR 1 — TERMINALS 1 & 2
" 2 — TERMINALS 2 & 5
" 3 — TERMINALS 3 & 4

Figure 17. Optical Micrograph of Diffused Silicon Resistor Network

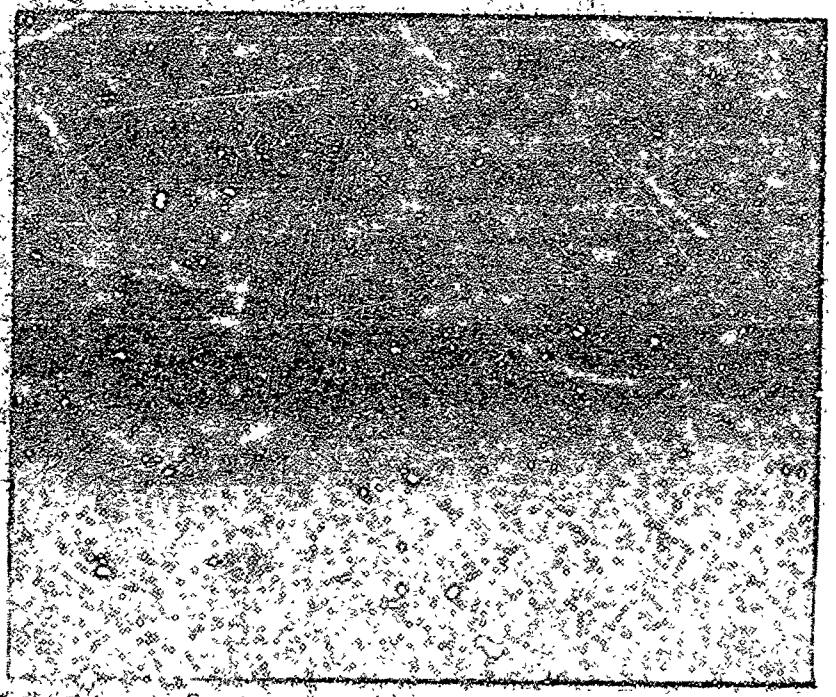

(LOCK HORIZONTAL)

Figure 18. Contact No. 1, Resistor No. 1. Negative Contact to Silicon Showing Hillocks and Whisker Growth

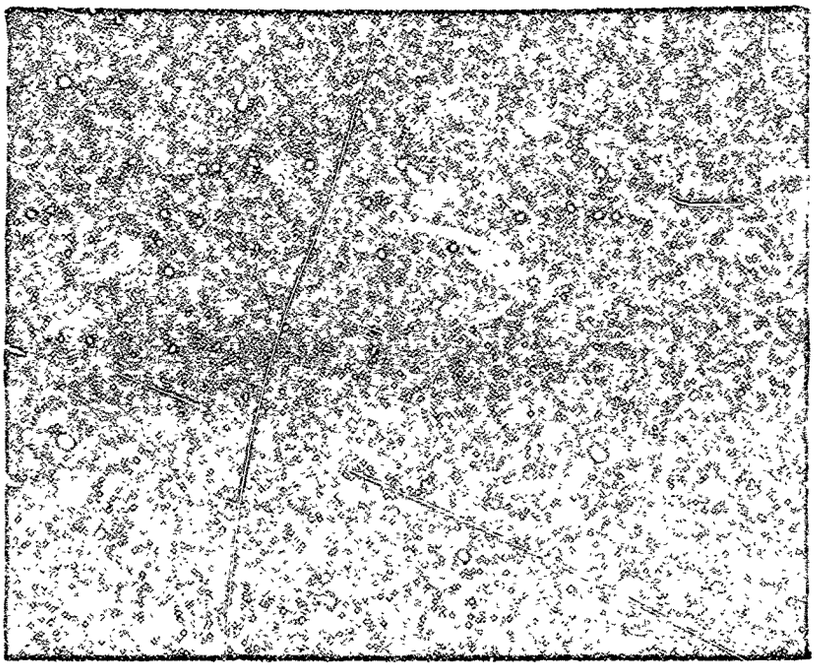

(2400X HORIZONTAL)

Figure 19. Aluminum Metallization Near Positive Aluminum Contacts to Diffused Silicon Resistors After Aging

An overall view of the negative contacts (4 and 5) is presented in Figure 20 showing extensive whisker and nodular growth near these contacts. One whisker has grown greater than 5.5 mils long and obviously could be a source of failure by electrically shorting to other conductors. An enlarged view of a negative contact area to a silicon diffused resistor is shown in Figure 21. The hillocks appear to be extruded aluminum while the whiskers are probably formed by aluminum ions condensing at screw dislocations. The diameter of the 5.5-mil long whisker measures 0.05 mil (1.25 microns).

Aluminum films which have been stressed in the absence of temperature gradients, current density gradients or compositional gradients form voids or hillocks uniformly distributed along the conductor length. In the presence of such gradients, however, voids grow rapidly at positive gradients and hillocks at negative gradients. A qualitative description of these is given above. Due to lack of time, a quantitative study of the effect of these gradients on failure was not possible and is recommended as a subject for future study.

2.3 ETCH PIT GROWTH IN SILICON DUE TO THE MASS TRANSPORT OF SILICON THROUGH ALUMINUM BY MOMENTUM EXCHANGE WITH CONDUCTING ELECTRONS

A failure mode associated with aluminum-silicon contacts is the growth of etch pits into silicon at the positive terminals during high current density and temperature stress. To show this effect, the aluminum conductor pattern was etched from the silicon diffused resistor samples described in Figures 17 through 21 of Section 2.2. "B" etch was used for 3 hours at room temperature to

(625 X HORIZONTAL)

Figure 20. Scanning Electron Micrograph of Aluminum Hillock and Whisker Growth Near Negative Terminals to Diffused Resistors. One whisker is nearly 5.5 mils long!

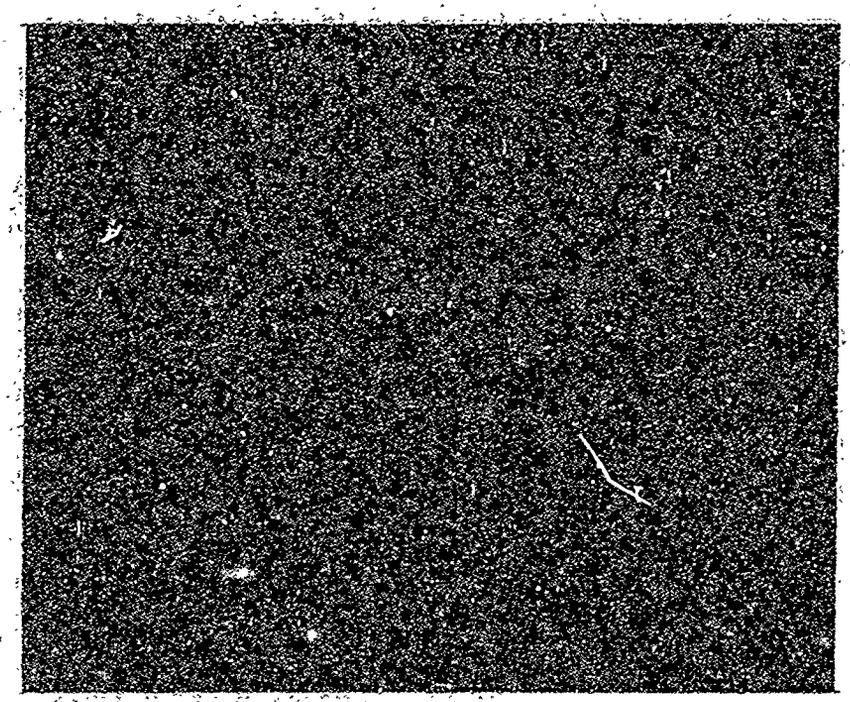

(2400X HORIZONTAL)

Figure 21. Enlarged View of Hillock and Whisker Structure Near Negative Contacts to Diffused Silicon Resistors

remove the aluminum 3-percent silicon conductor metal.

"B" Etch Formula: 2 parts of volume, distilled water
1 part nitric acid
1 part acetic acid
16 parts phosphoric acid

A scanning electron beam photomicrograph of the three positive contacts to the three resistors is shown in Figure 22. All contact areas exhibit rectangular or square etch pits into the <100> oriented silicon. An enlarged view of the center positive contact is presented in Figure 23. This is the positive contact from terminal No. 2 on resistor No. 2 as identified in Figure 17. Some material is also seen to be on top of the silicon surface and is probably silicon which was initially deposited as a 3-percent alloy with the aluminum conductor.

The etch pit formation is due to:

(a) Solid state dissolution of silicon into aluminum to saturate the aluminum at its operating temperature.
(b) Transport of the dissolved silicon away from the interface by momentum exchange between thermally activated silicon ions and conducting electrons enabling further solid state dissolution of silicon into the aluminum.

At 235°C, about 0.003 weight percent of silicon can exist in solid solution with the aluminum. The silicon from the substrate at both positive and negative terminals dissolves into the aluminum to satisfy this solubility limit. The activation energy for the

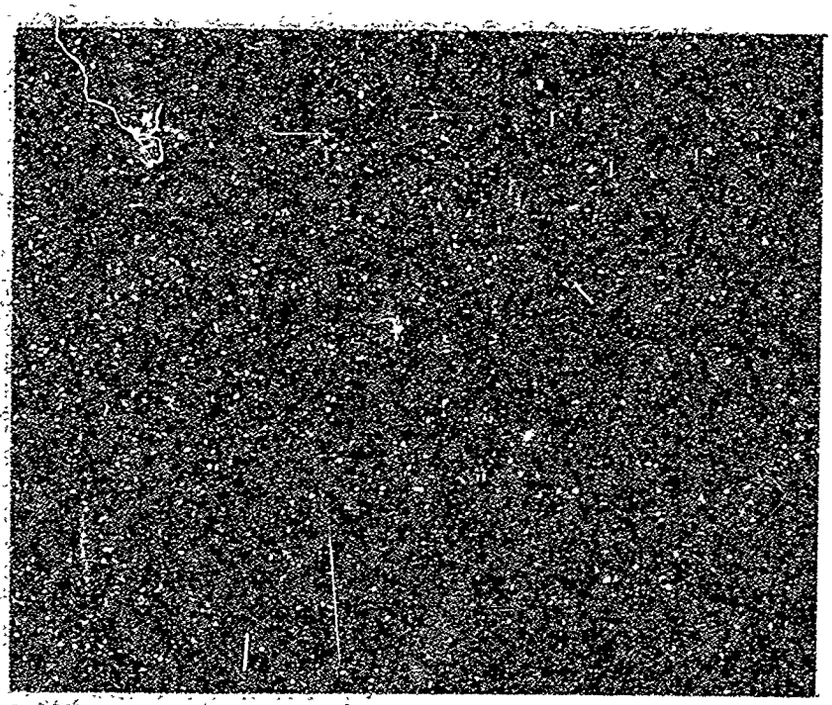

(1260 X HORIZONTAL)

Figure 22. Positive Silicon Contact Areas After Aging and Removal of Aluminum Showing Etch Pits in <100> Oriented Silicon

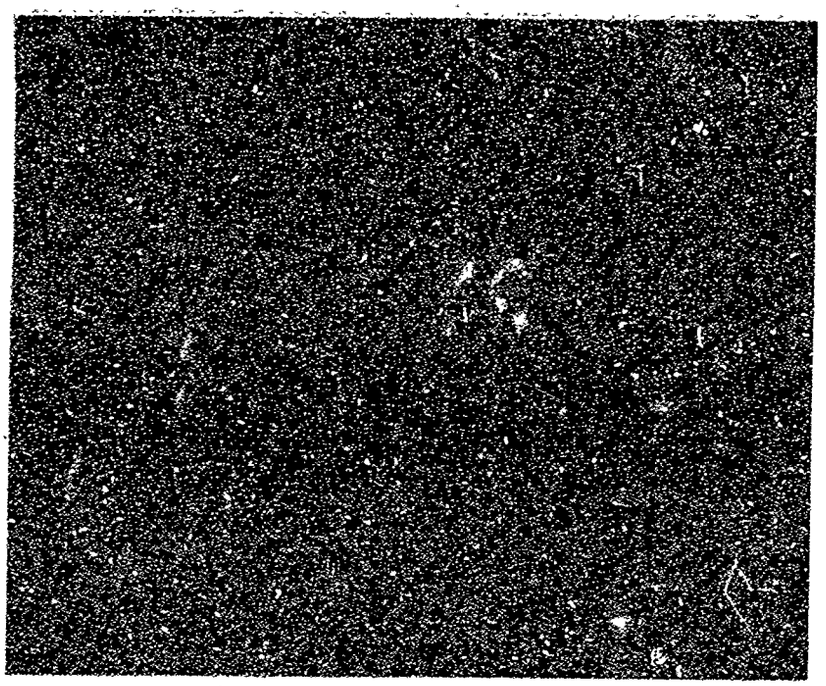

(6,500X HORIZONTAL)

Figure 23. Enlarged View of Positive Silicon Contact After Stress and Removal of Aluminum Conductor Showing Rectangular Etch Pits in <100> Oriented Silicon

diffusion of silicon into aluminum (estimated to be about 0.95 ev)[8] is lower than that of aluminum in aluminum (1.4 eV). It is expected, then, that the silicon in solid solution is readily activated and at the positive terminal is swept away from the interface by the force due to the rate of momentum exchange between the activated silicon ions and the conducting electrons. More silicon from the substrate is then able to dissolve into the aluminum where it is again swept downstream by the electrons. Because silicon will preferentially enter the aluminum from crystalline dislocations, rather than uniformly over the interface, the process results in the formation of etch pits into the silicon at crystalline dislocations. The process can continue until the junction beneath the aluminum-silicon contact interface is electrically shorted by growth of an etch pit through the junction.

Figure 24 shows two negative contact areas to silicon after stress and removal of the aluminum conductor. These are contacts No. 4 and 5 leading to resistors No. 2 and 3, as identified by Figure 17. An enlarged view of one of these silicon contact interfaces is shown in Figure 25. No etch pits into the silicon are observed at these contacts. A growth of crystallites is observed, however, on the surface of the silicon at these interfaces and is attributed to silicon which was initially deposited with the aluminum film being transported down the aluminum conductor stripe to this interface.

Etch pits are not formed in the negative silicon contact areas because the silicon which was initially dissolved into the aluminum remains supersaturated at this interface by means of the mass transport mechanism preventing further dissolution of silicon into aluminum.

---

(8) From Data Presented by C. Schnable, R. Keen, L. Lowenstern, "Study of Contact Failures in Integrated Circuits," Technical Report No. RADC-TR-67-331, Sept. 1967.

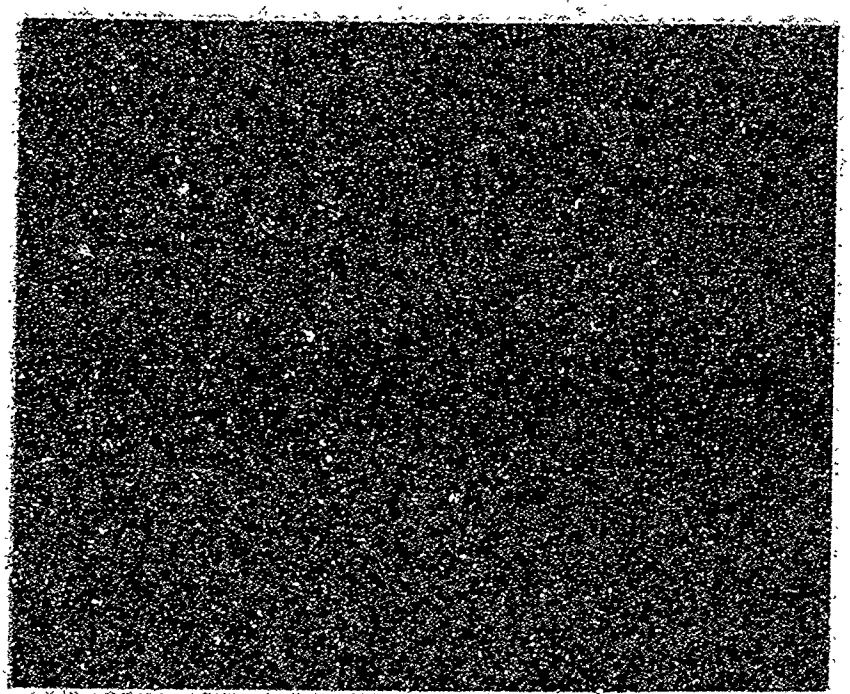

(2,800X HORIZONTAL)

Figure 24. Two Negative Contact Areas to Silicon After Stress and Removal of the Aluminum Conductor Shows No Etch Pits and Growth of Silicon Crystallites Due to Mass Transport of Silicon Codeposited with the Aluminum

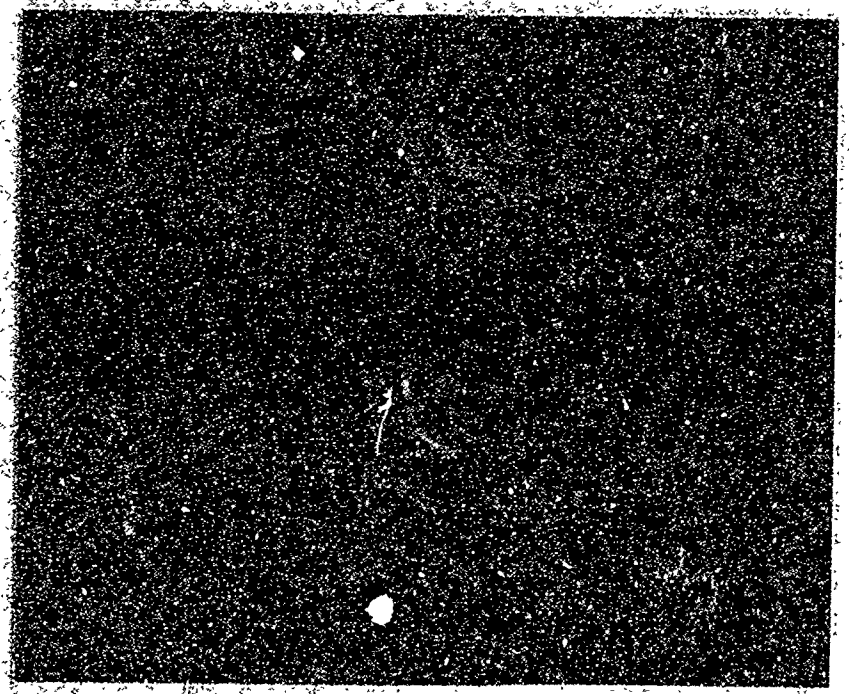

(6,300X HORIZONTAL)

Figure 25. Enlarged View of Negative Contact Area to Silicon After Removal of Aluminum Showing Absence of Etch Pits and the Growth of Silicon Crystallite due to Mass Transport of Silicon Codeposited with the Aluminum

It should be pointed out that the mass transport [illegible] of silicon in aluminum can lead to the etching of aluminum conductors into silicon. Aluminum conductors supported on silicon and carrying high current densities parallel to the silicon-aluminum interface can transport dissolved silicon away from the silicon-aluminum interface and deposit it at supersaturated regions of the conductor as silicon crystallites. The process can continue forming etch pits into the silicon and crystallites of silicon distributed throughout the aluminum. Such an effect was recently described but not explained by C. B. Oliver.[(9)]

In the above discussion a qualitative description of the etch pit formation into silicon at positive aluminum-silicon contacts carrying high current densities at elevated temperatures has been presented. Due to lack of time, a quantitative determination of the etch pit growth rate as a function of current density and temperature has not been possible and is a subject recommended for future study.

2.4 ALUMINUM-1-PERCENT-SILICON WIRE FAILURE

During the experimental evaluation of large-area-crystallite, thick aluminum films coated with a 7000 Å thick layer of glass, it was observed that two cells of devices failed due to bonding wire failure rather than due to film failure. The films under stress were thick (12,000 Å) and wide (1.43 mils) which due to their large cross-sectional area required currents in excess of 0.5 ampere to reach film current densities near 1.2 million amperes per square centimeter. The bonding wires were 1 mil diameter aluminum, 1 percent silicon and the test was carried out using dc current in an oven set at 140°C.

---

(9) C. B. Oliver, "Dagradation of Evaporated Aluminum Contacts on Silicon Planar Transistors," Sixth Annual Reliability Physics Symposium Proceedings, 11. 209-215, IEEE Catalog No. 7-15C58

Table VII presents the test conditions for these wires along with their mean-time-to-failure. It is estimated that the wire temperature exceeded 400°C during this test.

TABLE VII

WIRE FAILURE DATA

Group	Current (Amperes)	Wire Current Density (Amperes/cm^2)	Mean Time to Failure (Hours)	Oven Temperature (°C)
1-3	0.532	1.05×10^5	1070	140
2-3	0.555	1.095×10^5	690	140

Figures 26 and 27 show photomicrographs of the wires observed after life testing. The life tests took place in hermetically sealed units in a nitrogen ambient. The magnification is 300X.

Figure 26 shows a typical "bamboo" structure of the wire with grain boundaries running across the wire diameter. The surface is restructured showing nodular growth which appears quite frequently, but not necessarily, at grain boundaries. There is a single crystal section of the wire near the center of this micrograph which is darker than others. This crystallite appears to be coated with a gray metallic material.

Figure 27 shows a somewhat kinked section of wire with a small crystallite growing out of the surface of the wire near the center of the photograph.

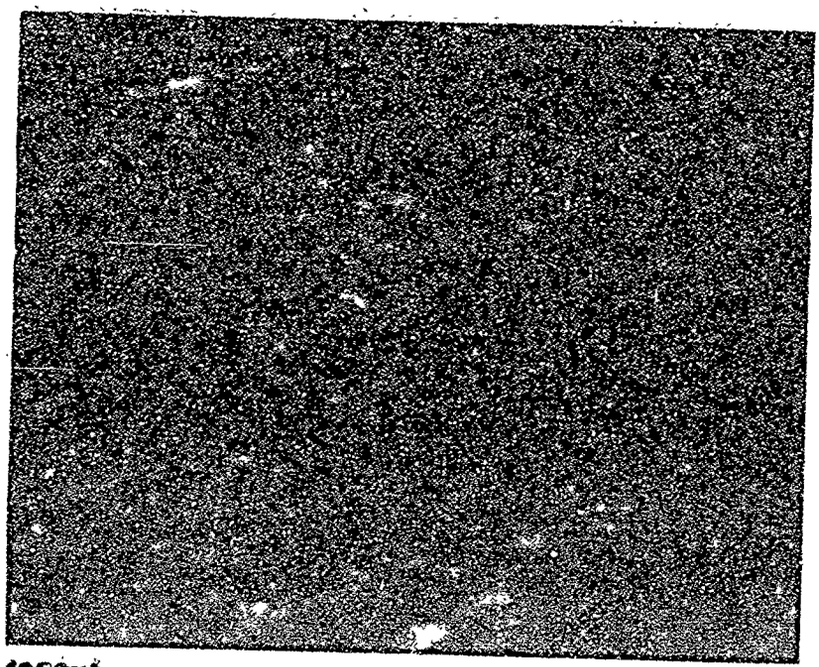

(300X)

Figure 26. Bambooed and Nodulated Al-1% Si Wire

(500X)

Figure 27. Bambooed and Kinked Wire with Nodules

Figure 28 is a micrograph of a badly kinked section of wire which appears to have first recrystallized to form a "bamboo" like structure and then melted at the grain boundaries enabling the wire to relieve any bending or compressional stress. The straight sections are single crystals of aluminum. Nodules often appear at the grain boundaries.

Scanning electron beam micrographs have also been obtained of a similar wire failure and are presented in the following: Figure 29 shows a view of the negative lead which had burned out near the bonding post and remained bonded to the aluminum stripe. The dark circular object in the background is a glass seal for the negative bonding post of the TO-5 header. It is seen that the aluminum has "bambooed" in that single crystals have grown sufficiently large to extend across the entire wire diameter. A spherical object appears near the break and appears to have been molten at one time. During aging of this sample, the electron flow was down the wire to the aluminum thin film.

Figure 30 shows an enlarged view of one of the grain boundaries (the second grain boundary above the "knee"). Ridges are observed to have formed in the wire surface. The crystal grain boundary extends across the wire cross section.

Figure 31 presents a view of the "kink" or "knee" in the wire as observed in Figure 29. Again, ridges appear on the surface of the wire extending across grain boundaries.

Figure 32 shows a view of the thermocompression bond between the aluminum-1-percent-silicon wire and a large-grained aluminum thin film, vacuum deposited on a silicon dioxide surface. An enlarged view of the crystallites which grow out of the surface of the wire is shown in Figure 33. By sectioning and evaluating

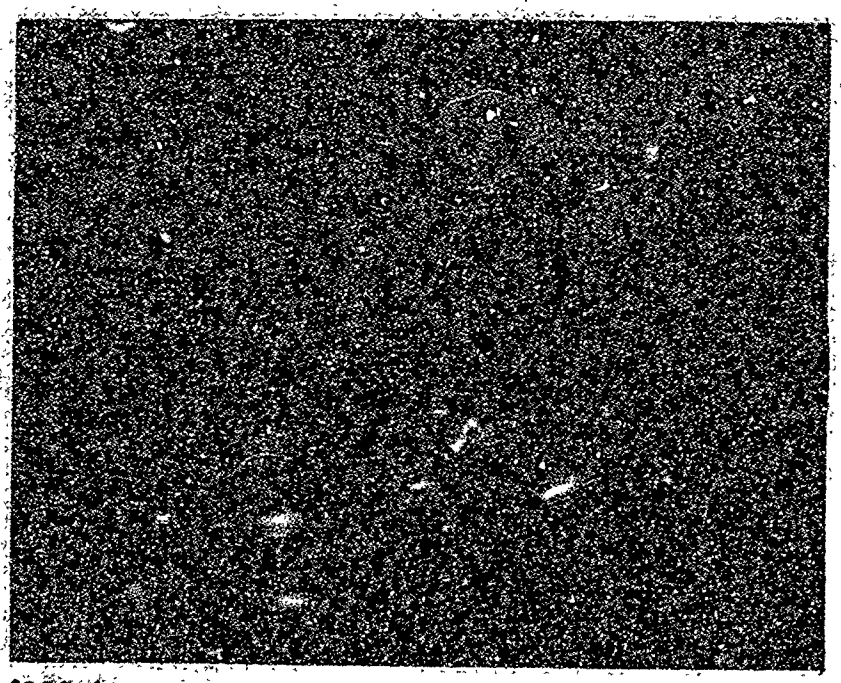

(300X)

Figure 28. Kinked Wire with Nodules

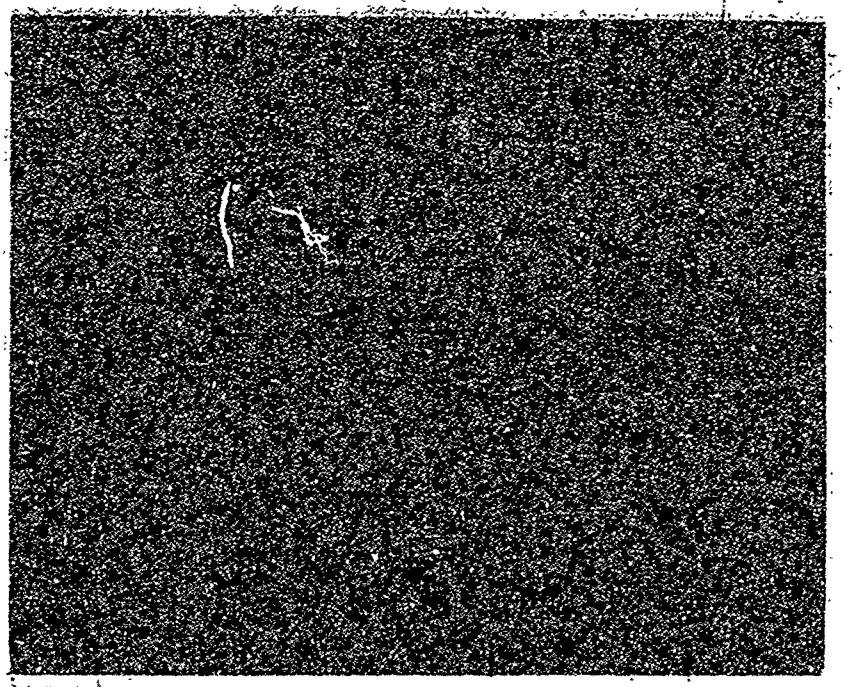

(120X)

Figure 29. Aluminum-1-Percent-Silicon Bonding Wire After 1.5×10^5 A/cm^2 Stress in a 140°C Oven for 900 Hours

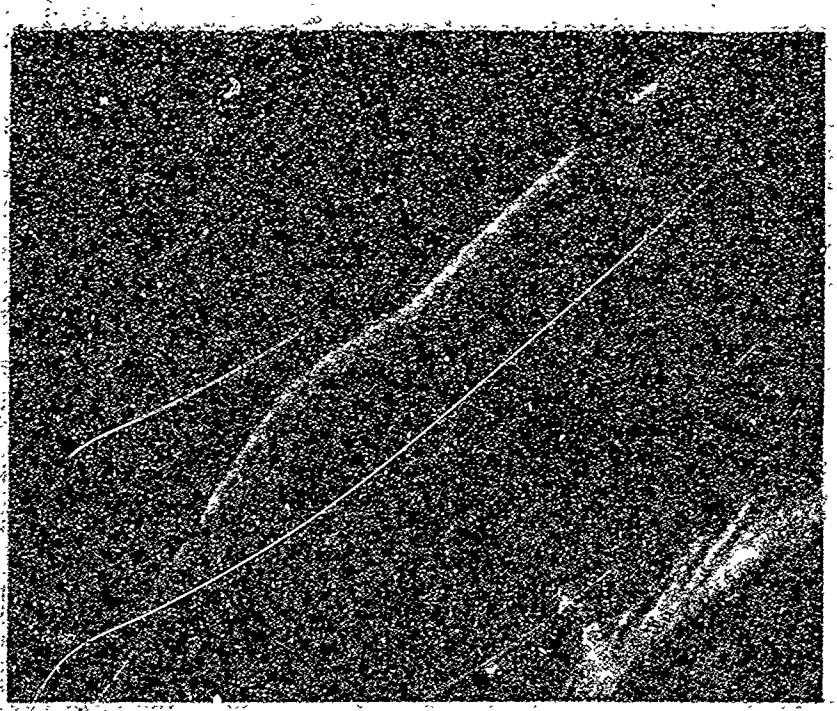

(2400X)

Figure 30. Aluminum-1-Percent-Silicon Wire After Stress Showing a Grain Boundary Extending Across the Wire Diameter

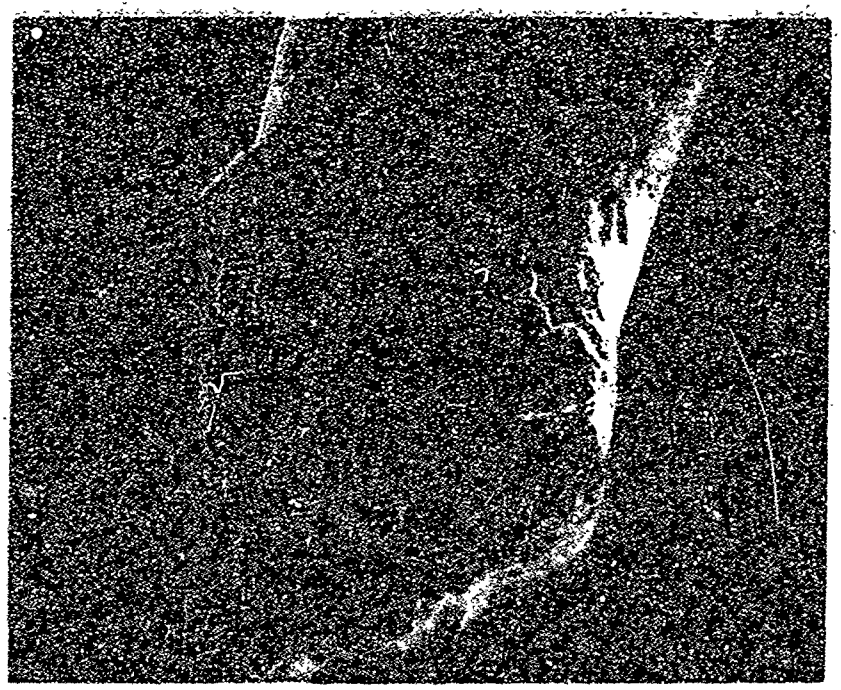

(2400X)

Figure 31. Enlarged View of Nodular Growth on Stressed Aluminum-1-Percent-Silicon Wire

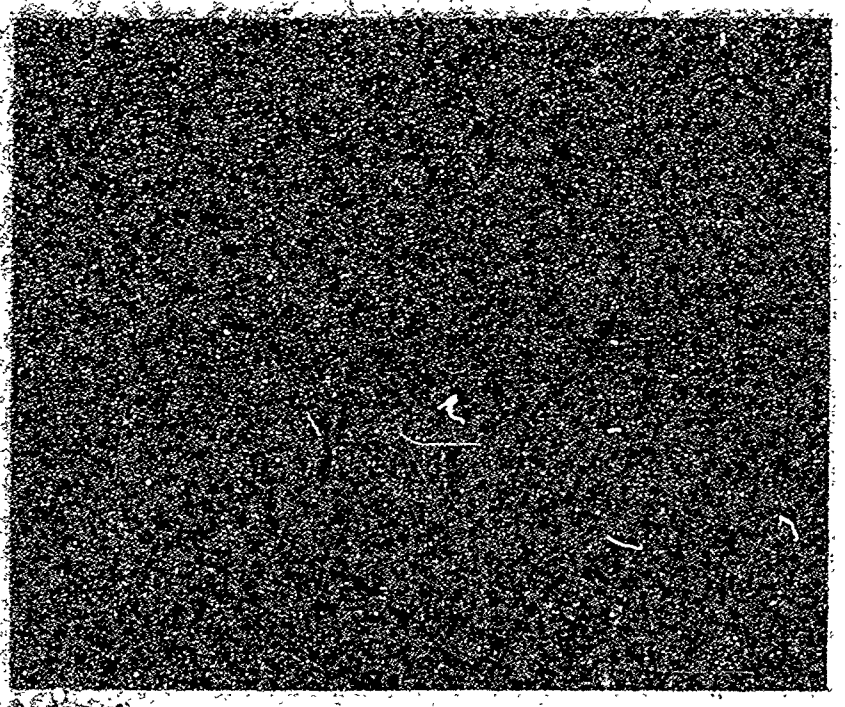

(1300X)

Figure 32. Micrograph of Thermocompression Bond Area Between a 1-mil Diameter Aluminum-1-Percent-Silicon Wire and an Aluminum Thin Film After Stress (Negative Terminal)

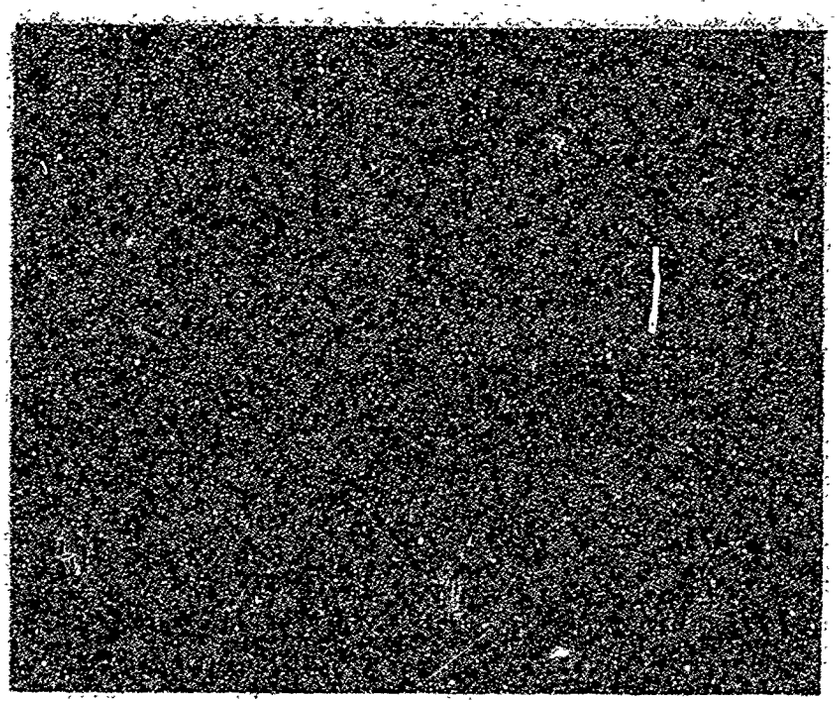

(2600X)

Figure 33. Enlarged View of Bond Area Showing Crystallite Growth (Negative Terminal)

similar cyrstallites by optical microscopy, it has been determined that the crystallites are considerably harder than aluminum and when etched appear to be silicon. It is concluded that the crystallites are silicon which has been transported down the aluminum-1-percent-silicon wire by momentum exchange with conducting electrons. A portion of the silicon dissolves into the aluminum to form a solid solution of silicon in aluminum. The diffusion coefficient of silicon in aluminum is greater than the self-diffusion coefficient of aluminum; silicon is, therefore, transported more readily down the aluminum wire by this mechanism than is aluminum. When the silicon ions reach the heat sink and cooler die supporting the aluminum film, the rate of transport of the silicon decreases, resulting in a super-saturated condition causing the silicon crystals to precipitate out of solution.

The observations made in this scanning electron beam microscopic investigation confirm observations made in Section 2.3 that silicon does dissolve into aluminum and is capable of mass transport through the aluminum by momentum exchange between thermally activated silicon ions and conducting electrons.

2.5 REACTION BETWEEN ALUMINUM AND SILICON DIOXIDE

The free energy change in the reaction

$$Al + SiO_2 \rightarrow Al_2O_3 + Si$$

is -150 kilocalories per mole at 500°C indicating that the reaction will proceed. The reaction is used extensively by the semiconductor industry to make ohmic contacts to silicon through the 20 to 30 Å thick SiO_2 films which naturally form over silicon at room temperature. To obtain processing design data enabling the silicon device engineer to choose time and temperatures for making ohmic contacts through the thin silica layers as well as to determine what role

this reaction may play in the degradation of the reliability of devices operated below 200°C, an experiment was designed to determine both the activation energy for this reaction and an equation relating the depth of penetration into the silica as a function of time and temperature.

Large crystallite well-ordered aluminum films were deposited onto 9600 Å thick thermally grown SiO_2 on silicon wafers. The deposition was made in a vacuum in the low 10^{-8} Torr region using 99.999 percent aluminum evaporated from tungsten filaments. The substrate temperature was maintained at 475°C during the deposition to promote the formation of well-ordered large-grained films. The aluminum film thickness ranged between 3400 and 4600 Å. A conductor stripe pattern was then etched into the aluminum providing conductor widths of 0.5, 1, 1.5 and 2 mils wide by 54 mils long.

Each wafer with the aluminum stripe pattern was broken into several pieces. The pieces from one wafer were placed into a furnace for aging for different times at a fixed temperature under a nitrogen ambient. The furnace temperature varied ±3°C over the muffle region in which the pieces were placed.

The depth of the reaction into the aluminum was determined by first exposing the region through the aluminum film and into the glass by shallow angle lapping of the structure as shown in Figure 34. The remaining glass thickness was determined by light interference patterns. The depth of penetration of the reaction was then readily determined from this information and from knowledge of the initial glass thickness.

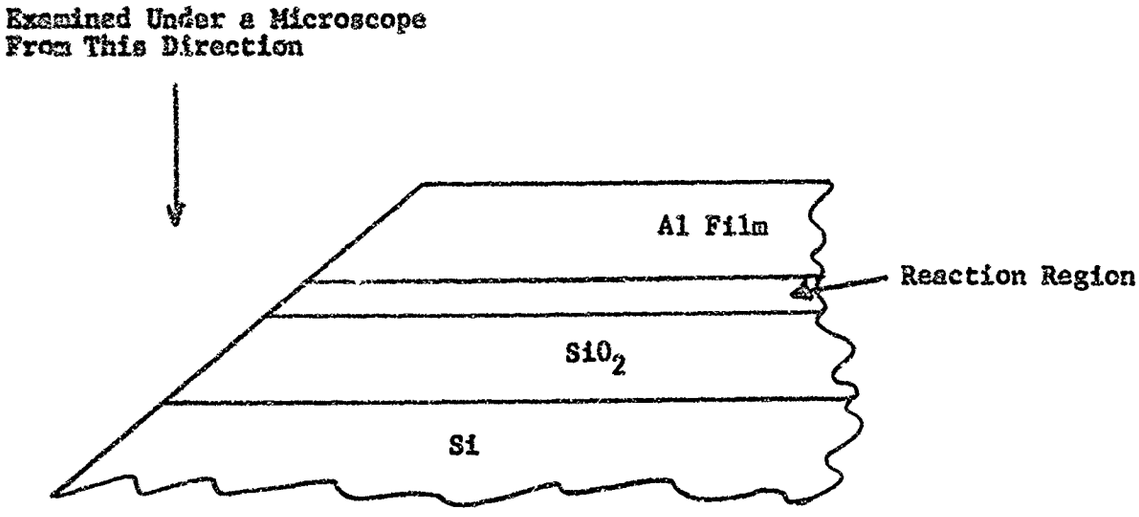

Figure 34. Cross-Sectional Diagram of Beveled Al on SiO_2 on Si Sample

Figure 35 presents photomicrographs of the angle lapped specimens aged at 523°C, indicating how the depth of penetration of the reaction was observed. In these views, the silicon base is to the left and appears to be finely scratched by the angle lapping process. Interference patterns due to white light are observed running through the glass wedge and parallel to the glass silicon interface. The interaction region appears dark and is seen to penetrate further into the glass as the aging time increases. It is also seen that under certain areas of the aluminum little reaction has taken place and is due to the formation of locally continuous layers of Al_2O_3 which prevent further reaction.

Figure 36 presents a plot of the depth of penetration of the reaction into the glass as a function of time for samples held at 543°, 533°, 523°, 513°, 503°, 463°, and 421°C. From the slopes of these experimental lines the rates of penetration of the reaction into glass were determined in angstroms per minute and are listed in Table VIII. An Arrhenius plot of this data showing a ln R vs $\frac{1}{°K}$ is given in Figure 37 from which the equation that describes the rate of reaction was determined to be: $R = 3.18 \times 10^{17} \exp -(2.562/kT)$ where R is expressed as angstroms per minute and k is 8.617×10^{-5} eV/°K/atom.

TABLE VIII

RATE OF ALUMINUM PENETRATION INTO SiO_2

Temperature (°C)	$\frac{1}{°K}$	Rate (A/min)
543	1.225	49.0
533	1.241	27.8
523	1.256	19.7
513	1.272	11.8
503	1.289	8.33
463	1.359	1.02
421	1.441	0.076

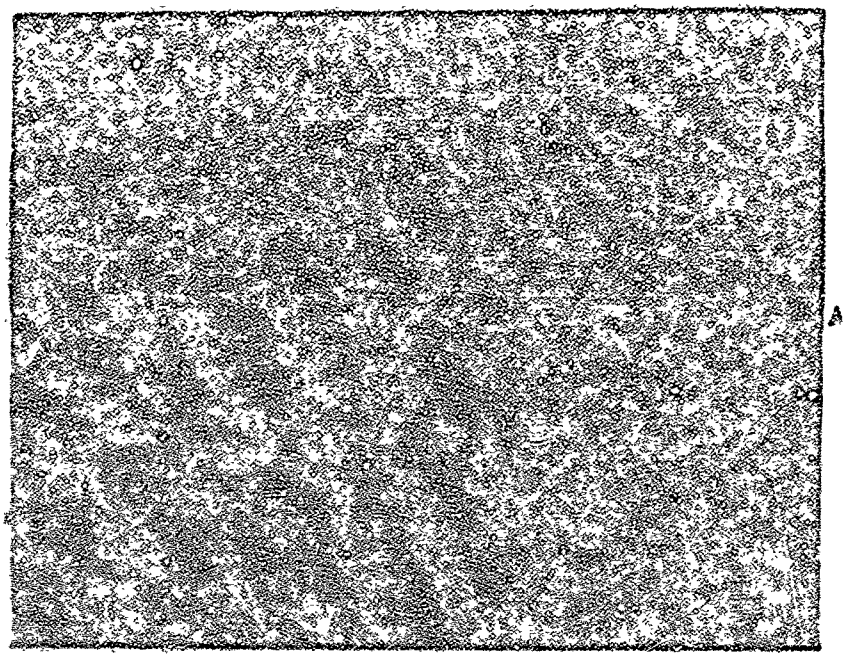

(270X) (a) 1-3/4 hours

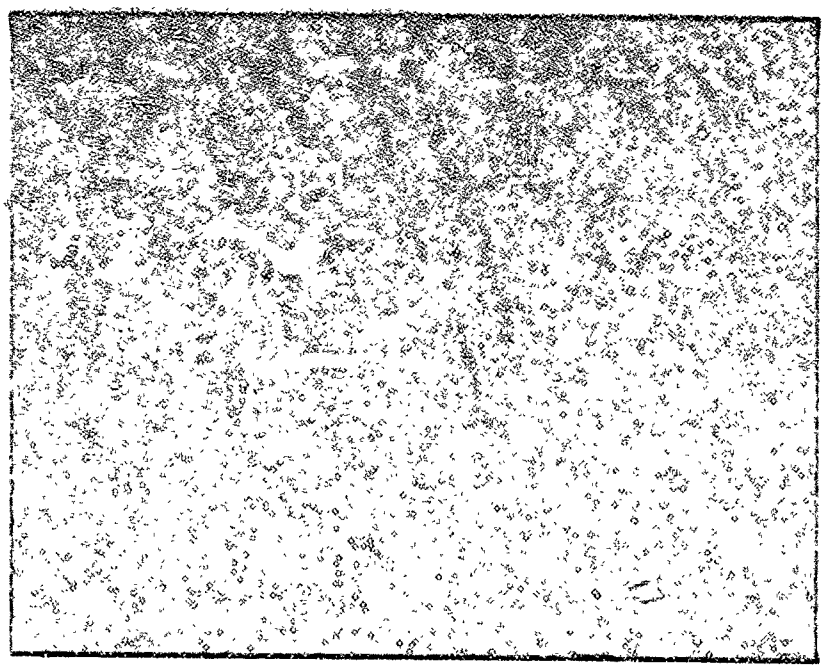

(270X) (b) 3 hours

Figure 35. Beveled Al on SiO_2 on Si Samples Aged at 523°C

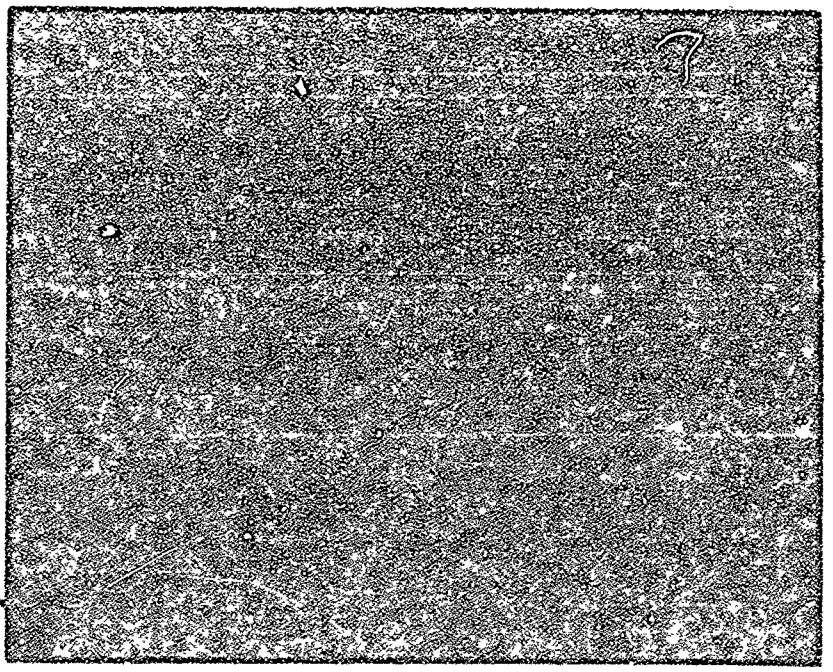

(270X)

(c) 4-1/2 hours

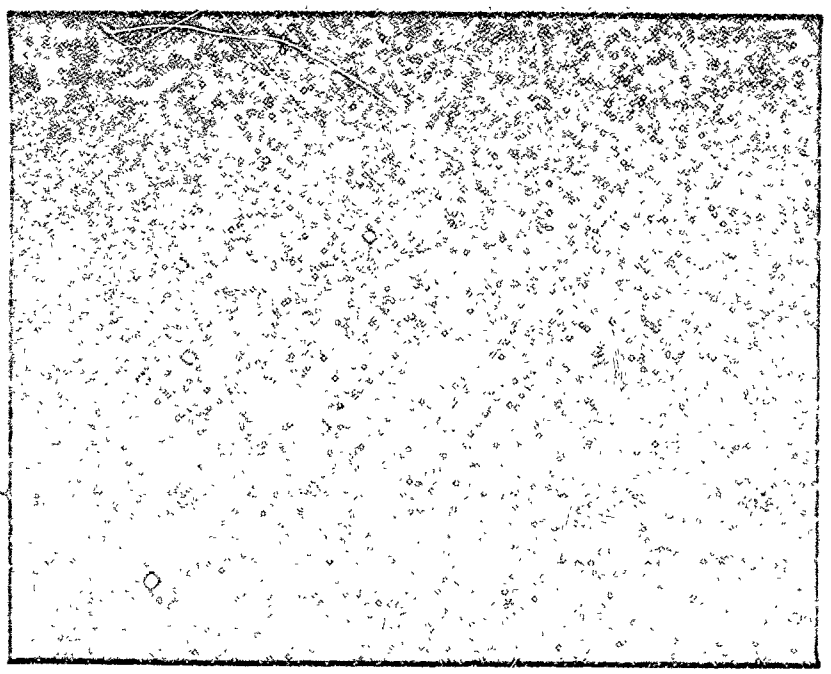

(270X)

(d) 6 hours

Figure 35 (continued). Beveled Al on SiO_2 on Si Samples Aged at 523°C

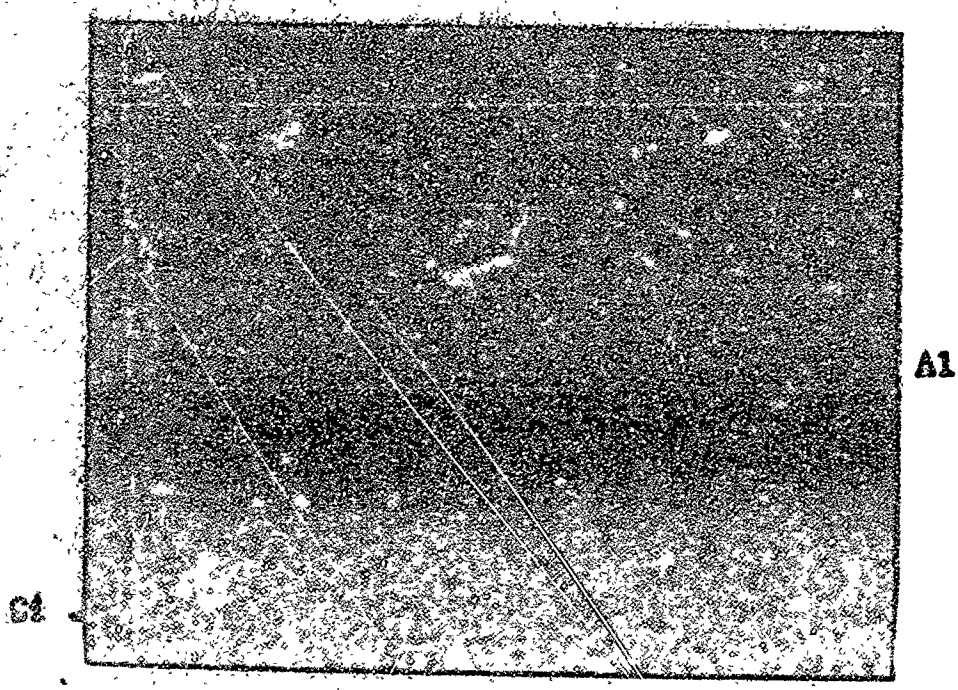

(a) 7-1/2 hours

Figure 35(continued). Evolved Al on SiO_2 on Si Aged at 523°C

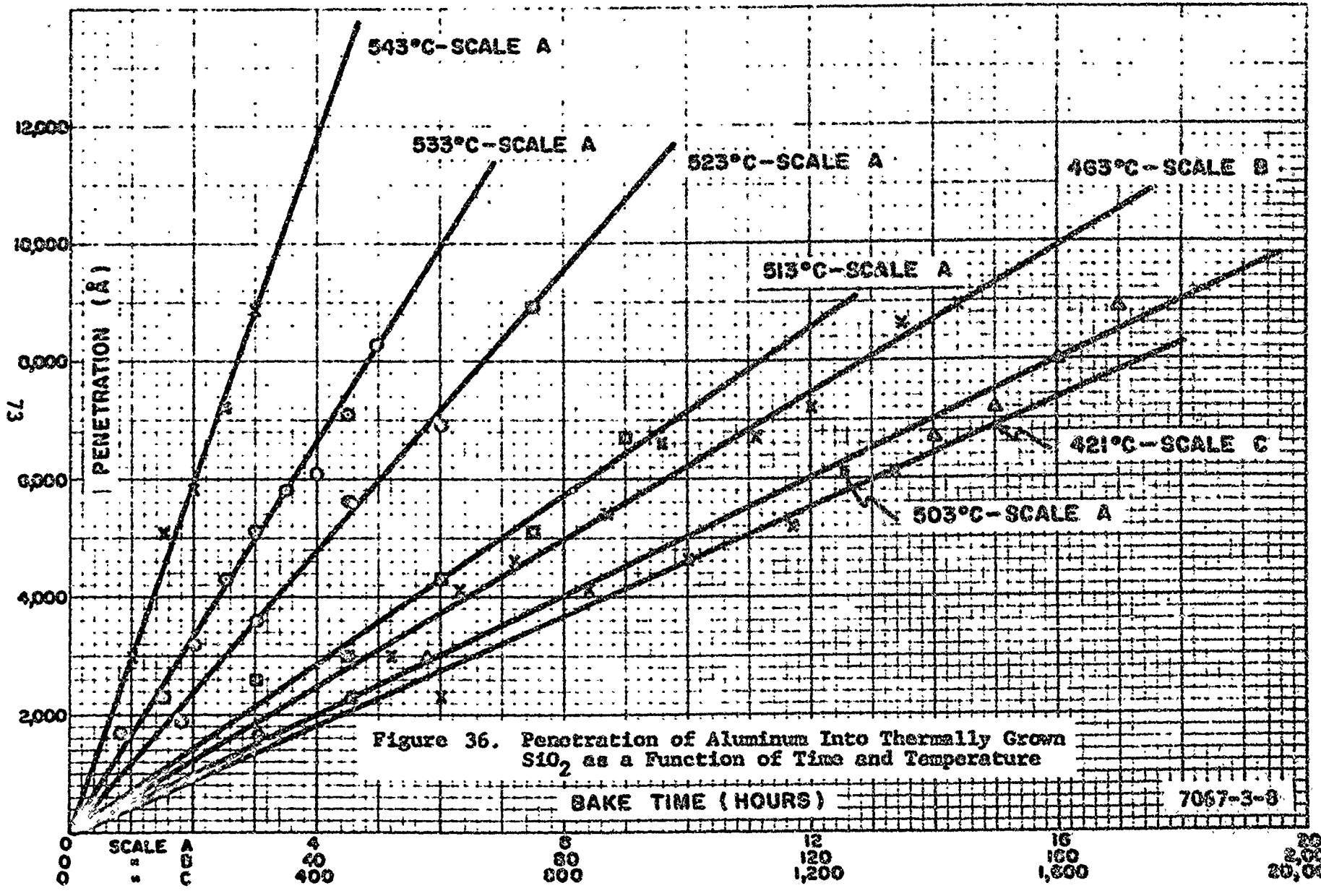

Figure 36. Penetration of Aluminum Into Thermally Grown SiO_2 as a Function of Time and Temperature

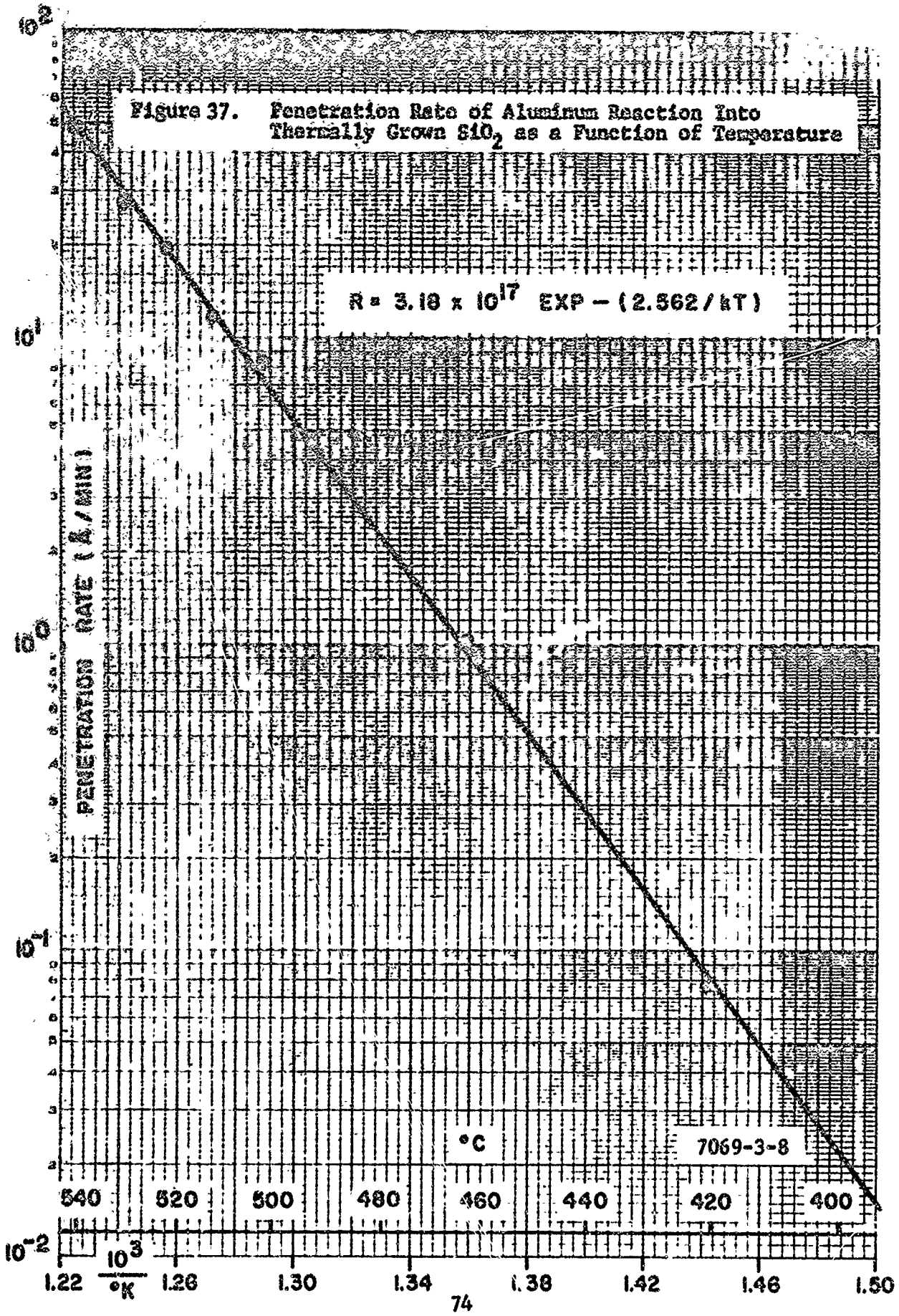

Figure 37. Penetration Rate of Aluminum Reaction Into Thermally Grown SiO_2 as a Function of Temperature

Figure 38 presents an extrapolation of the data to lower temperatures and is valid only if the reaction obeys the above derived formula at the lower temperatures. It is seen from this figure that at 340°C the penetration rate is 1.9×10^{-4} A/min which is the rate required to penetrate 1000 Å of glass in 10 years. It is also seen that this mode of failure is not a significant one at the operating temperature range of semiconductor devices below 200°C.

2.6 DISSOLUTION OF SILICON INTO ALUMINUM

Due to the solid solubility of silicon into aluminum, the latter can act as an etchant for silicon at relatively low temperatures where the process takes place by solid state diffusion. The etching of silicon by aluminum, like other etches, is not uniform and preferentially attacks crystalline defects to form etch pits. These etch pits can traverse through shallow p-n junctions causing failure by an electrical short.

The region of solid solubility is indicated in the metallurgical phase diagram of this system presented by Hansen[10] shown in Figure 39. The region of interest is enlarged in the insert which shows the solubility to fall off from a maximum at 577°C to near zero at below 300°C.

The amount of silicon removed by dissolution into aluminum at a given temperature is determined by the solid solubility and the amount of aluminum available. The data given by Hansen[10] for the solubility curve which he considered to be most accurate was generated by Dix and Heath[11] in 1928 using micrographic area analysis. The materials used by these investigators were:

---

(10) M. Hansen, Constitution of Binary Alloys, 2nd Edition, McGraw-Hill Book Company, Inc., 1958.

(11) E. H. Dix and A. C. Heath, Trans. A.I.M.E., 78, 1928, 164-194.

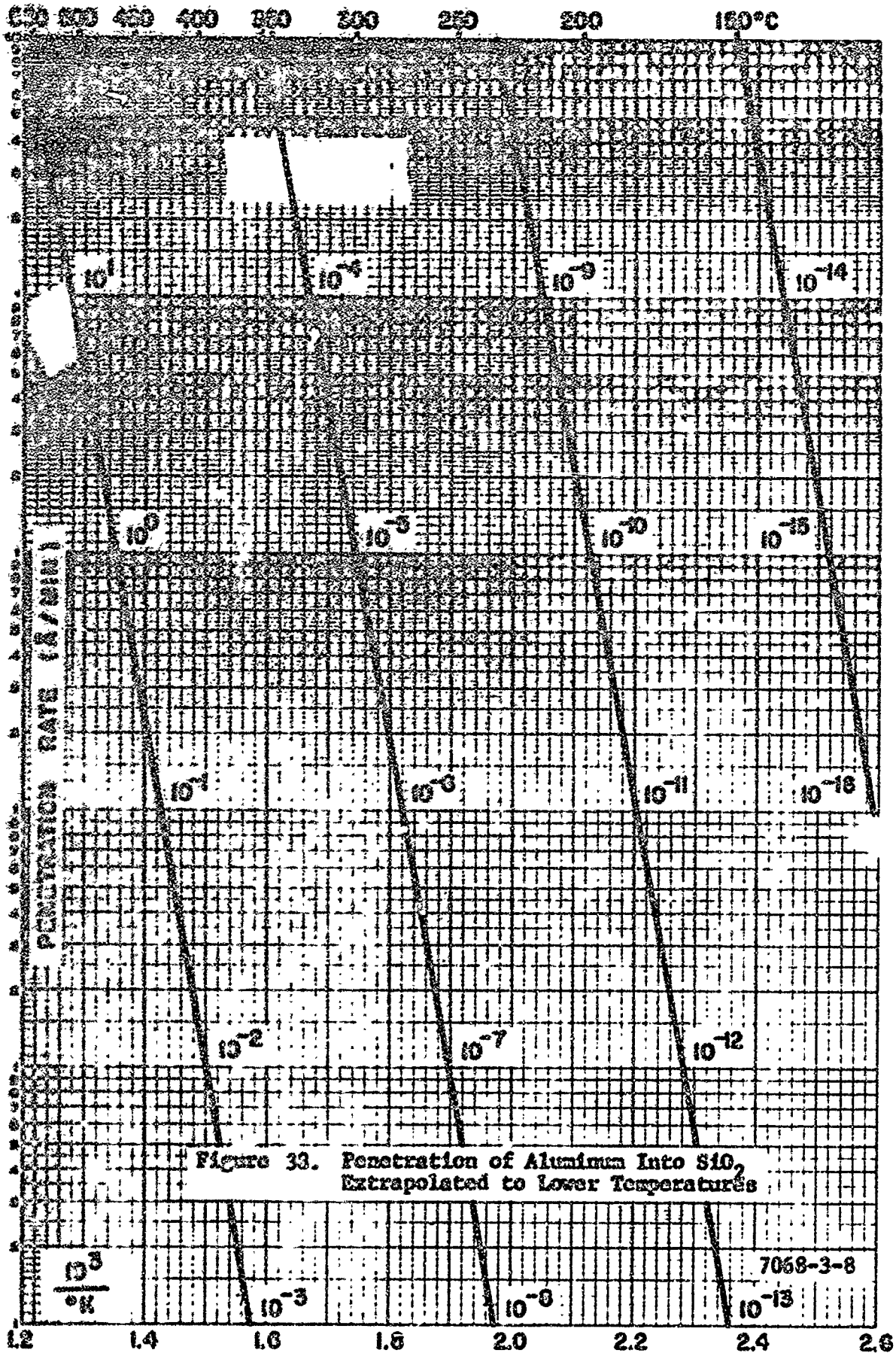

Figure 33. Penetration of Aluminum Into SiO_2 Extrapolated to Lower Temperatures

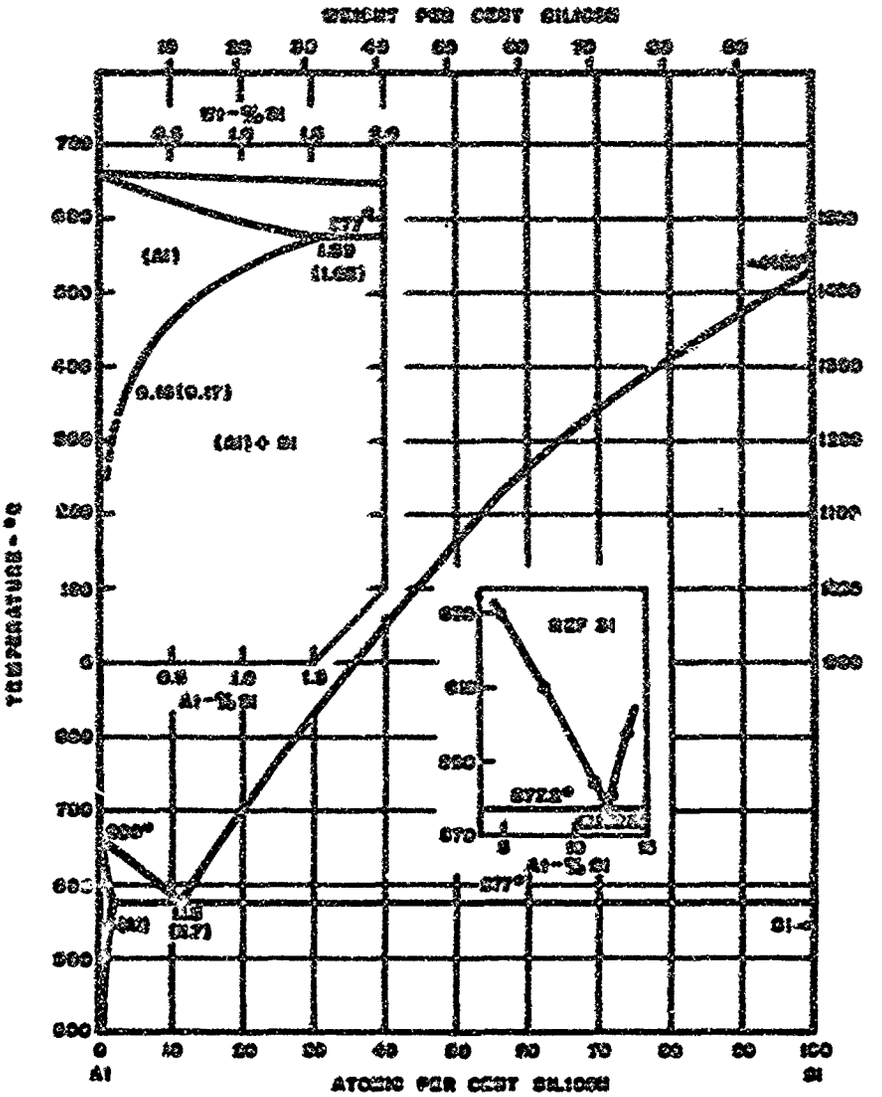

Figure 39. Aluminum-Silicon Phase Diagram

Al%	Cu%	Fe%	Si%	Mn%	Ti%	V%
99.951	0.021	0.012	0.013	nil	0.002	0.001

and

Si%	Cu%	Fe%	Mn%	Al%	Ti%
98.64	nil	0.66	0.04	0.56	0.01

An experiment was therefore designed to update this data utilizing materials of high purity. The method chosen was to determine the weight percent of silicon dissolved into aluminum that has been vacuum deposited onto silicon.

Silicon wafers were:

(1) cleaned
(2) weighed to ±3 micrograms
(3) coated with vacuum deposited Al (99.999%) on both sides
(4) weighed to ±3 micrograms
(5) heat treated
(6) etched to remove Al with dissolved Si
(7) weighed to ±3 micrograms.

The method, however, proved to be inaccurate due to oxidation effects of the Al and Si during heat treatment and was abandoned. It is recommended that the establishment of the solid-solubility curve of silicon into aluminum employing pure materials be the subject of a future study.

SECTION III

3.0 CONCLUSIONS

The results of a 15-month study of potential failure modes of aluminum on silicon semiconductor devices have been presented. The major effort was devoted to studies of the mass transport of aluminum by momentum exchange with conducting electrons and to the reaction between aluminum and silicon dioxide. Qualitative information has also been generated concerning the mass transport of silicon through aluminum by momentum exchange with conducting electrons leading to etch pit formation in silicon at those contacts where electrons leave the silicon and enter the aluminum. Also, micrographs have been obtained showing structural changes in overstressed aluminum wires used to contact semiconductor surfaces. An attempt to establish the solid-solubility curve for silicon in aluminum using pure elements was not successful.

3.1 MASS TRANSPORT OF ALUMINUM BY MOMENTUM EXCHANGE WITH CONDUCTING ELECTRONS

The mean-time-to-failure for aluminum conductor stripes which possess no gradients in temperature, current density or composition that are stressed at high current densities and elevated temperatures can be expressed as

$$\frac{1}{J^2 \, MTF} = \frac{A}{w\,t} \exp -(\phi/kT)$$

or

$$MTF = \frac{w\,t}{A\,J^2} \exp (\phi/kT)$$

where MTF = mean-time-to-failure in hours

J = current density in amperes per square centimeter

k = 8.62×10^{-5} eV/atom/°K

T = film temperature in degrees Kelvin

A = constant

ϕ = activation energy in electron volts

w = film width in cm

t = film thickness in cm.

The activation energy for this failure mode has been determined for highly polycrystalline, well-ordered large crystalline and glassed well-ordered large crystalline films. The activation energy is identical to that for the lattice self-diffusion of aluminum in aluminum modified by factors involving both surface diffusion and grain boundary diffusion. These latter two factors can be important in films formed by the condensation of aluminum vapor.

Large-grained well-ordered aluminum films overcoated by a layer of deposited glass exhibit values of

ϕ = 1.2 eV

and A = 8.5×10^{-10}

Large-grained (about 8-micron lateral dimension) well-ordered aluminum films are characterized by

ϕ = 0.84 eV

and A = 5×10^{-18}

Small crystallite (about 1.2-micron lateral dimensions) show values of

ϕ = 0.48 eV

and A = 2.43×10^{-16}

At film temperatures of 275°C and above, the physical structure of the aluminum film is not an important factor in determining lifetime since in that temperature range all film structures follow the formula which expresses the lifetime for well-ordered and glassed films. This is because at 275°C and above, aluminum diffusion through the crystal lattice predominates over grain boundary diffusion and surface diffusion.

At temperatures below 275°C the film structure becomes important in determining conductor lifetime. At 100°C nearly three orders of magnitude improvement in lifetime can be achieved through the use of well-ordered glassed films in place of highly polycrystalline nonglassed films.

Due to inaccuracies in film temperature measurement and to the small cell size of these experiments an accurate experimental determination of the power for J cannot be obtained even though the value of J has been varied over a range in excess of 5:1. A statistical analysis of the data, however, indicates that the exponent of J is definitely not unity and exceeds the value of two by only a small amount. At this time the exponent value of 2 for J appears to be valid but further work is required to substantiate this.

3.2 MASS TRANSPORT OF ALUMINUM AT ALUMINUM-SILICON CONTACTS

Temperature gradients, current density gradients and compositional gradients can establish locations within the conductor where vacancies can rapidly cluster to form a void and thus degrade the lifetime as predicted by the equations discussed in Section 3.1. Voids form at positive gradients while aluminum

hillocks and whiskers grow at negative gradients (in terms of electron flow). Whiskers could be a cause of failure if they grow sufficiently long to short to nearby conductors.

More time is required to establish formulas which predict lifetime of aluminum conductors which contain such gradients when stressed at high current densities and temperatures. It is recommended that this be the subject of further study.

3.3 ETCH PIT FORMATION IN SILICON DUE TO THE MASS TRANSPORT OF SILICON THROUGH ALUMINUM BY MOMENTUM EXCHANGE WITH CONDUCTING ELECTRONS

It has been shown that etch pits grow in silicon at high current density silicon-aluminum contacts where electrons leave the silicon and enter the aluminum. This is due to

(1) Solid state diffusion of silicon into aluminum to saturation at the contact temperature.

(2) Transport of the dissolved silicon away from the silicon-aluminum interface by momentum exchange between thermally activated silicon and conducting electrons to permit further dissolution of silicon into the aluminum.

Etch pits form in the silicon by this means only at those contacts where the dissolved silicon is swept away from the junction and through the aluminum by the "electron wind." Thus, etch pits do not grow by this method at aluminum-silicon contacts where the electrons enter the silicon since the "electron wind" maintains saturation conditions by keeping the dissolved silicon in the vicinity of the interface.

Time was not available to determine the rate of etch pit growth normal to the surface as a function of current density and temperature. It is recommended that this study be made in the near future since it is a potential failure mode for shallow junction devices.

3.4 MICROSCOPIC INVESTIGATION OF ALUMINUM-1-PERCENT-SILICON WIRE FAILURE

Micrographs have been presented showing gross structural change leading to wire failure of 1-mil diameter aluminum bonding wires containing 1-percent silicon when stressed at elevated temperatures and current densities. It was also shown that silicon is transported through such wires in the direction of electron flow.

3.5 REACTION BETWEEN ALUMINUM AND SILICON DIOXIDE

An equation which describes the rate of aluminum transport into silicon dioxide by reduction of the silicon dioxide to silicon has been determined to be:

$$R = 3.18 \times 10^{17} \exp - (2.562/kT)$$

where R = rate of penetration into SiO_2 in angstroms per minute
k = 8.62×10^{-5} eV/atom/^{o}K
T = temperature of the couple in degrees Kelvin.

At operating temperatures of 200^{o}C this reaction rate is insignificant and therefore is not a failure mode at that temperature. During processing, however, at elevated temperatures this reaction could be a precurser to a failure mode. The high activation energy for this reaction of 2.562 eV makes the reaction rate most sensitive to temperature.

3.6 DISSOLUTION OF SILICON INTO ALUMINUM

A method chosen to establish the solid-solubility curve for pure silicon into pure aluminum failed to be sufficiently accurate. It is recommended that additional effort be placed on this project since the best currently available data was obtained with nonpure materials in 1928. It is an important factor in the formation of etch pits into silicon at silicon-aluminum interfaces when those interfaces are subjected to elevated temperatures and could be a source of failure for shallow junction devices.

UNCLASSIFIED
Security Classification

DOCUMENT CONTROL DATA - R & D

(Security classification of title, body of abstract and indexing annotation must be entered when the overall report is classified)

1. ORIGINATING ACTIVITY (Corporate author) Motorola, Inc., Semiconductor Products Division, 5005 E. McDowell Road, Phoenix, Arizona 85008	2a. REPORT SECURITY CLASSIFICATION UNCLASSIFIED 2b. GROUP N/A

3. REPORT TITLE

METALLIZATION FAILURES IN INTEGRATED CIRCUITS

4. DESCRIPTIVE NOTES (Type of report and inclusive dates)

Final 28 Dec 66 to 27 Apr 68

5. AUTHOR(S) (First name, middle initial, last name)

James Black

6. REPORT DATE	7a. TOTAL NO. OF PAGES	7b. NO. OF REFS
October 1968	84	

8a. CONTRACT OR GRANT NO.	9a. ORIGINATOR'S REPORT NUMBER(S)
F30602-67-C-0166 b. PROJECT NO. 5519 c. Task 551906 d.	9b. OTHER REPORT NO(S) (Any other numbers that may be assigned this report) RADC-TR-68-243

10. DISTRIBUTION STATEMENT

This document is subject to special export controls and each transmittal to foreign governments, foreign nationals or their representatives may be made only with prior approval of RADC(EMERP), GAFB, NY 13440.

11. SUPPLEMENTARY NOTES	12. SPONSORING MILITARY ACTIVITY
	Rome Air Development Center (EMERP) Griffiss Air Force Base, New York 13440

13. ABSTRACT

The activation energy for the mass transport of aluminum by momentum exchange with conducting electrons has been obtained and equations relating temperature, current density, film structure, and film geometry to conductor life are presented. The conductor lifetime is shortened if thermal gradients, current density gradients, or compositional gradients exist. Void formation at a compositional gradient where electrons leave silicon and enter aluminum has been qualitatively studied. Also, it is shown that that hillocks and whiskers of aluminum form at aluminum-silicon interfaces when electrons leave aluminum and enter silicon. Etch pit growth into silicon at silicon-aluminum contacts carrying high current densities where electrons leave the silicon and enter aluminum has been qualitatively studied. Two concurrent mechanisms leading to the formation of these etch pits are: (1) the dissolution of silicon into aluminum to reach near saturation, and (2) the transport of the dissolved silicon ions down the aluminum and away from the interface by momentum exchange with conducting electrons. A microscopic study of aluminum wires containing 1-percent silicon is presented showing gross structural changes when stressed at elevated current densities. Silicon is also shown to be transported down the wires in the direction of electron flow. Equations relating the rate of penetration of aluminum into silicon dioxide to temperature are presented. This reaction is shown to be unimportant as a failure mode at normal device operating temperatures of 200°C and below.

DD FORM 1 NOV 65 1473

UNCLASSIFIED
Security Classification

Security Classification

14. KEY WORDS	LINK A		LINK B		LINK C	
	ROLE	WT	ROLE	WT	ROLE	WT
Aluminum						
Metallization of Integrated Circuits						
Electromigration						
Failure Mechanisms						
Al - Si Interaction						
Al - SiO_2 Interaction						

UNCLASSIFIED

Security Classification